

SUSCEPTIBILITY OF MID-RISE AND HIGH-RISE STEEL MOMENT  
RESISTING FRAME BUILDINGS TO THE NONLINEAR BEHAVIOR OF  
BEAM-COLUMN CONNECTIONS

A THESIS SUBMITTED TO  
THE GRADUATE SCHOOL OF NATURAL AND APPLIED SCIENCES  
OF  
MIDDLE EAST TECHNICAL UNIVERSITY

BY

MURAT BAYRAKTAR

IN PARTIAL FULFILLMENT OF THE REQUIREMENTS  
FOR  
THE DEGREE OF MASTER OF SCIENCE  
IN  
CIVIL ENGINEERING

OCTOBER 2017



Approval of the thesis:

**SUSCEPTIBILITY OF MID-RISE AND HIGH-RISE STEEL MOMENT  
RESISTING FRAME BUILDINGS TO THE NONLINEAR BEHAVIOR OF  
BEAM-COLUMN CONNECTIONS**

submitted by **MURAT BAYRAKTAR** in partial fulfillment of the requirements for  
the degree of **Master of Science in Civil Engineering Department, Middle East  
Technical University** by,

Prof. Dr. Gülbin Dural Ünver  
Dean, Graduate School of **Natural and Applied Sciences**

\_\_\_\_\_

Prof. Dr. İsmail Özgür Yaman  
Head of Department, **Civil Engineering**

\_\_\_\_\_

Prof. Dr. Afşin Sarıtaş  
Supervisor, **Civil Engineering Dept., METU**

\_\_\_\_\_

**Examining Committee Members:**

Prof. Dr. Cem Topkaya  
Civil Engineering Dept., METU

\_\_\_\_\_

Prof. Dr. Afşin Sarıtaş  
Civil Engineering Dept., METU

\_\_\_\_\_

Assoc. Prof. Dr. Özgür Kurç  
Civil Engineering Dept., METU

\_\_\_\_\_

Assoc. Prof. Dr. Ozan Cem Çelik  
Civil Engineering Dept., METU

\_\_\_\_\_

Asst. Prof. Dr. Saeid Kazemzadeh Azad  
Civil Engineering Dept., Atılım University

\_\_\_\_\_

**Date:** 23.10.2017

**I hereby declare that all information in this document has been obtained and presented in accordance with academic rules and ethical conduct. I also declare that, as required by these rules and conduct, I have fully cited and referenced all material and results that are not original to this work.**

Name, Last name: Murat Bayraktar

Signature :

## **ABSTRACT**

### **SUSCEPTIBILITY OF MID-RISE AND HIGH-RISE STEEL MOMENT RESISTING FRAME BUILDINGS TO THE NONLINEAR BEHAVIOR OF BEAM-COLUMN CONNECTIONS**

Bayraktar, Murat

M.S., Department of Civil Engineering

Supervisor: Prof. Dr. Afşin Sarıtaş

October 2017, 82 pages

Moment resisting steel frames provide significant energy dissipation capacity in the event of a major seismic excitation. In order to ensure this, one of the most critical regions to pay attention is the beam-column connections, where their behavior is greatly simplified and idealized for the purpose of design in practice. In this thesis, the variables inherent in steel connections are taken into account through a parametric study by considering both static push-over analysis and nonlinear time history analysis. There has been research on this topic especially for low-rise buildings, but for mid-rise and particularly high-rise buildings, the effects of connection nonlinearity, such as strength loss and pinching in response, as well as the design approach of structural system, is not investigated in detail through a parametric nonlinear time history analysis. In order to undertake this effort, OpenSees structural analysis program is considered, where force-based frame element with fiber discretization is adopted to capture spread of inelasticity along element length and section depth. Connection behavior is introduced through a hysteretic model that can consider strength loss and pinching effects. The selected mid-rise and high-rise buildings have perimeter moment resisting frames, where these are analyzed in the plane. The effects of internal gravity frames are taken into account through the use of lean-on-columns.

Nonlinear geometric effects on all columns are considered through the use of corotational transformation. For the time history analysis 2 set of 20 ground motions that are scaled for 10% and 2% probability of exceedance in 50 years are imposed on the structure. Inter-story drift ratio profiles and base shear versus roof drift ratio responses of the structures are examined. Limit states considered in the specifications are taken into account in order to assess the significance of connection nonlinearity on overall structural system response. It is concluded that the influence of nonlinear behavior at beam-column connections yields less increase in structural drift demands on mid-rise to high-rise structures than those observed in low-rise structures. Furthermore, as long as ductility of connections is ensured, semi-rigid behavior of connections provide energy dissipation, and still maintain the structural response of mid-rise and high-rise steel moment resisting frame structures within limits.

Keywords: Moment resisting steel frames, Nonlinear time history analysis, Beam-column connections, Mid-rise building, High-rise building

## ÖZ

### **ORTA VE YÜKSEK KATLI MOMENT AKTARAN ÇELİK ÇERÇEVE BİNALARIN KOLON-KİRİŞ BAĞLANTILARIN DOĞRUSAL OLMAYAN DAVRANIŞINA KARŞI OLAN DUYARLILIĞININ ARAŞTIRILMASI**

Bayraktar, Murat

Yüksek Lisans, İnşaat Mühendisliği Bölümü

Tez Yöneticisi: Prof. Dr. Afşin Sarıtaş

Ekim 2017, 82 sayfa

Moment aktaran çelik çerçeveler deprem durumunda önemli düzeyde enerji sönümlemesi sağlamaktadırlar. Bu özelliğin sağlanabilmesi için dikkat gösterilmesi gereken kısım, tasarım aşamasında davranışı basitleştirilmeye çalışılan kolon-kiriş bağlantılarıdır. Bu tezde, çelik bağlantılara ilişkin olan değişkenler doğrusal olmayan statik itme ve deprem verilerine göre zaman tanım alanında analizler kullanılarak parametrik bir çalışmayla gerçekleştirilmiştir. Bu konuda alçak katlı binalar için araştırma yapılmış olsa da, bağlantıların kapasite kaybı ya da çevrimsel davranışlarında daralma gibi doğrusal olmayan davranışlarının neden olacağı etkiler orta ve yüksek katlı binalarda detaylı olarak özellikle de zaman alanında dinamik parametrik analiz yürütülerek gerçekleştirilmemiştir. Analizleri yürütmek için OpenSees programı kullanılmış, yapı elemanları boyunca ve kesitlerinde dağılmış olan plastikleşmeyi modellemek için kuvvet bazlı çerçeve elemanları kullanılmıştır. Bağlantıların doğrusal olmayan davranışını modellemede kapasite kaybı ve çevrimsel davranışta daralma gözönünde bulundurulmuştur. Analizlerde dikkate alınan orta ve yüksek katlı binalardaki moment aktaran çerçevelerin çözümleri düzlemde gerçekleştirilmiştir. İçerde kalan ve moment aktarmayan çerçevelere etkiyen düşey

yüklerin ve kütlelerin etkisi fiktif kolon vasıtasıyla moment aktaran çerçeveye yansıtılmıştır. Yüksek yanal deplasmanlarda kolonlardaki doğrusal olmayan geometrik etkileri dikkate almak için korotasyonel geometrik dönüşüm kullanılmıştır. Zaman tanım alanında doğrusal olmayan analiz için 50 yılda %10 aşılma olasılığı ve 50 yılda %2 aşılma olasılığı ile ölçeklendirilmiş yirmişer deprem kaydı bulunan iki set kullanılmıştır. Bağlantıdaki doğrusal olmayan davranışın yapısal sistem üzerindeki etkisini ölçebilmek için şartnamelerde belirlenen öteleme seviyeleri gözönünde bulundurulmuştur. Yarı-rijit bağlantıların doğrusal olmayan davranışının orta ve yüksek katlı binalarda alçak katlılara göre daha az yapısal talep yarattığı yürütülen çalışmanın ve karşılaştırmaların sonucunda görülmüştür. Bağlantıların sünek davranışı sağlandıkça, bağlantıların yarı-rijit davranışının enerji sönmülemesi sağladığı, ve orta ve yüksek katlı çelik çerçeve yapıların sistem davranışına limitleri aşmayan etki yarattığı tespit edilmiştir.

Anahtar Kelimeler: Moment aktaran çerçeveler, Zaman tanım aralığında doğrusal olmayan dinamik analiz, Kolon-kiriş bağlantıları, Orta katlı binalar, Yüksek katlı binalar

## ACKNOWLEDGEMENTS

I would like to express my deepest gratitude to my supervisor Prof. Dr. Afşin Sarıtaş for his guidance and patience throughout this study.

I thank to my friends Güven Aldırmaz, Okan Çağrı Bozkurt, Yusuf Tolga Mutlu, Emre Erdem, Umut Akın, Serdar Bahar, Mehmet As, Gürel Baltalı, Erman Bigikoçin, Armağan Adıgüzel, Zafer Karakaş, Ali Can Tatar, Eren Burak Tutuş, Mert Karadağlı and Önder Alparslan. I also thank to Hüseyin Alpdünder, Celal Yaşam Öner, Uygur Karadeniz for their support and friendship in Oman.

Finally, I am deeply grateful to my family.



## TABLE OF CONTENTS

ABSTRACT .....	v
ÖZ .....	vii
ACKNOWLEDGEMENTS .....	ix
TABLE OF CONTENTS .....	xi
LIST OF TABLES .....	xiii
LIST OF FIGURES .....	xv
LIST OF ABBREVIATIONS .....	xix

### CHAPTERS

INTRODUCTION .....	1
1.1 General .....	1
1.2 Moment Resisting Steel Frames .....	3
1.3 Partially Fixed Connections .....	4
1.3.1 Single Web-Angle and Single Plate Connections .....	4
1.3.2 Double Web-Angle Connections .....	5
1.3.3 Top and Seat Angle Connections with Double Web Angle .....	6
1.3.4 Extended End – Plate Connections and Flush End-Plate Connections .....	7
1.3.5 Header Plate Connections .....	8
1.4 Literature Survey .....	9
1.4.1 Proposed models for moment-rotation behavior of beam-column connections .....	9
1.4.1.1 Frey-Morris Polynomial Model .....	10
1.4.1.3 Three-Parameter Power Model .....	12
1.4.1.4 Cyclic moment-rotation models for steel connections .....	13
1.4.2 Studies on the effect of partially restrained connections on steel frames .....	13
1.5 Objectives and Scope .....	17
ANALYZED BUILDINGS .....	19

2.1 Description of the Buildings.....	19
2.2 Modeling Procedure .....	29
OVERVIEW OF STRUCTURAL ANALYSIS TYPES .....	41
3.1 Modal Analysis.....	41
3.2 Nonlinear Static (Push-Over) Analysis .....	41
3.3 Nonlinear Time History Analysis.....	44
4.1 Fundamental Periods of the Considered Buildings .....	51
4.2 Push-Over Analysis Results for the 9-Story Buildings .....	52
4.3 Push-Over Analysis Results for the 20-Story Building.....	55
4.3 Non-Linear Time History Analysis Results .....	57
4.4 Comparison with the Study of Karakas [50] .....	70
SUMMARY AND CONCLUSION .....	73
REFERENCES.....	77

## LIST OF TABLES

Table 1.1: Curve-Fitting Constants and Standardization Constants for Frye-Morris Polynomial Model (all size parameters are in centimeters) [48] .....	11
Table 2.1: Column and Beam Geometric Properties for LB design of 9-Story Building .....	W14 23
Table 2.2: Geometric Dimensions of Column Sections for W14 LB Design of 9 Story Building.....	24
Table 2.3: Geometric Dimensions of Girder (Beam) Sections for W14 LB Design of 9-Story Building.....	24
Table 2.4: Column and Beam Geometric Properties for UB Design of 9-Story Building.....	W36 24
Table 2.5: Geometric Dimensions of Column Sections for UB design of 9 Story Building.....	W36 25
Table 2.6: Beam Sizes for the W36 UB Design of 9 Story Building.....	25
Table 2.7: Column and Beam Geometric Properties for W14 Design of 20-Story Building.....	28
Table 2.8: Geometric Dimensions of Column Sections for W14 Design of 20-Story Building.....	29
Table 2.9: Geometric Dimensions of Girder (Beam) Sections for W14 Design of 20-Story Building .....	29
Table 2.10: Beam-Column Elements in Opensees [42] .....	31
Table 2.11: Connection Classification by Strength .....	35

Table 3.1: Los Angeles (LA) ground motions for the 10% in 50 years hazard .....	45
Table 3.2: Los Angeles (LA) ground motions for the 2% in 50 years hazard level ..	46
Table 3.3: Drift Ratios by Structural Performance Level for Steel Moment Frames in FEMA 356.....	48
Table 4.1: List of Models for the 9 Story Building.....	50
Table 4.2: List of Models for the 20 Story Building.....	51
Table 4.3: The First Periods of the 9 Story Building .....	51
Table 4.4: Maximum Median of IDR Values of the 9 Story Building.....	61
Table 4.5: Maximum of the 84th Percentile of IDR Values of the 9 Story Building	62
Table 4.6: Maximums of Median and of 84 <sup>th</sup> Percentile of IDR Values of the 20 Story Building.....	67
Table 4.7: Maximums of Median of IDR Values of the 3 Story Building by Karakas [50] .....	70
Table 4.8: Maximums of 84th percentile of IDR Values of the 3 Story Building by Karakas[50] .....	71

## LIST OF FIGURES

Figure 1.1: Elastic and Inelastic Design Spectrums.....	2
Figure 1.2: Typical Moment Resisting Frame [48].....	4
Figure 1.3: Single Web-Angle connection [48].....	5
Figure 1.4: Single Plate connection [48].....	5
Figure 1.5: Double Web-Angle [48].....	6
Figure 1.6: Top and Seat-Angle connection with a Double Web-Angle [48] .....	6
Figure 1.7: Extended End-Plate connection [48].....	7
Figure 1.8: Flush End-Plate Connection [48] .....	7
Figure 1.9: Header Plate Connection [48] .....	8
Figure 1.10: Moment Rotation Curves of The Typical Connections [48].....	8
Figure 2.1: Plan View of the 9-Story Building .....	20
Figure 2.2: Elevation View of 9-Story Building.....	21
Figure 2.3: Elevation View of 20-Story Building.....	26
Figure 2.4: Plan View of the 20-Story Building .....	27
Figure 2.5: Plan View and the Idealized Model of the 9-Story Building .....	33
Figure 2.6: Response of Hysterical Material Model in OpenSees [42] .....	34
Figure 2.7: Idealized Acceptable Response of a Connection in SMRF [48] .....	35

Figure 2.8: Fully restrained (FR), PR, and simple connections [48] .....	36
Figure 2.9: Defined Spring Model in OpenSees .....	38
Figure 2.10: Presentation of Mild and Severe Pinching Cases for Connection Response under Strength Loss Case .....	39
Figure 3.1: Typical Load Patterns for Push-Over Analysis .....	43
Figure 3.2: Response Spectra for the 1st set of Ground Motion Data .....	47
Figure 3.3: Response Spectra for the 2nd set of Ground Motion Data .....	47
Figure 4.1: Push-Over Curves for the Rigid Cases (LB and UB) .....	53
Figure 4.2: Push-Over Curves for the LB 9-Story Buildings without Strength Loss	54
Figure 4.3: Push-Over Curves for LB 9-Story Buildings with Strength Loss .....	55
Figure 4.4: Push-Over Curves for 20-Story Buildings without Strength Loss .....	56
Figure 4.5: Push-Over Curves for 20-Story Buildings with Strength Loss .....	57
Figure 4.6: Nonlinear Time History and Push-over Analyses Results for Rigid Buildings of 9-Story (Left) and 20-Story (Right) .....	58
Figure 4.7: Push-over Analysis (PA) and Nonlinear Time History Analysis (NTHA) Results of Model 17 for 9-Story Building subjected to LA40 (continuous curve: PA, dotted curve: NTHA) .....	59
Figure 4.8: IDR profiles of Models 1 and 3 of 9-Story Building .....	62
Figure 4.9: IDR profiles of Models 2 and 4 of 9-Story Building .....	63
Figure 4.10: IDR profiles of Models 5 and 7 of 9-Story Building .....	63
Figure 4.11: IDR profiles of Models 6 and 8 of 9-Story Building .....	63
Figure 4.12: IDR profiles of Models 9 and 11 of 9-Story Building .....	64

Figure 4.13: IDR profiles of Models 10 and 12 of 9-Story Building.....	64
Figure 4.14: IDR profiles of Models 13 and 15 of 9-Story Building.....	64
Figure 4.15: IDR profiles of Models 14 and 16 of 9-Story Building.....	65
Figure 4.16: IDR profiles of Models 17 and 19 of 9-Story Building.....	65
Figure 4.17: IDR profiles of Models 18 and 20 of 9-Story Building.....	65
Figure 4.18: IDR profiles of Models 21 and 23 of 9-Story Building.....	66
Figure 4.19: IDR profiles of Models 22 and 24 of 9-Story Building.....	66
Figure 4.20: IDR profiles of Models 25 and 26 of 9-Story Building.....	66
Figure 4.21: IDR profiles of Models 1 and 3 of 20-Story Building.....	68
Figure 4.22: IDR profiles of Models 2 and 4 of 20-Story Building.....	68
Figure 4.23: IDR profiles of Models 5 and 7 of 20-Story Building.....	68
Figure 4.24: IDR profiles of Models 6 and 8 of 20-Story Building.....	69
Figure 4.25: IDR profiles of Models 9 and 11 of 20-Story Building.....	69
Figure 4.26: IDR profiles of Models 10 and 12 of 20-Story Building.....	69



## LIST OF ABBREVIATIONS

$\beta$	Ratio of Peak Moment Capacity of Connection to the Plastic Moment Capacity of the Connecting Beam
$\lambda$	Ratio of Connection's Initial Stiffness to Flexural Rigidity of Connecting Beam
$\theta_s$	Rotation of a Connection at Service Loads
$A$	Area of Steel Section
$K_c$	Rotational Stiffness of Connection
$K_s$	Secant Stiffness of a Connection at Service Loads
$M_{ch}$	Post-Yielding Stiffness of Connection
$M_{cp}$	Peak Moment Capacity of Connection
$M_{cy}$	Yield Moment Capacity of Connection
$M_n$	Maximum Moment a Connection Able to Carry
$M_p$	Plastic Moment Capacity of a Beam
$R_\mu$	Ductility Reduction Factor
$R_o$	Overstrength reduction factor
$t_f$	Flange Thickness
$t_w$	Web Thickness
ATC	Applied Technology Council
CLE	Contingency Level Earthquake
CP	Collapse Prevention
FEMA	Federal Emergency Management Agency
FR	Fully Restrained
IDR	Interstory Drift Ratio
IMF	Intermediate Moment Frames
IO	Immediate Occupancy

LB	Lower Bound
LS	Life Safety
PR	Partially Restrained
UB	Upper Bound
UBC	Uniform Building Code

## CHAPTER 1

### INTRODUCTION

#### 1.1 General

Several simplifications are considered in order to ease the analysis and design stages of structures. One such simplification is the assumption that linear elastic analysis can be used for design. If structural members are to be designed to remain elastic in the event of a major seismic excitation, this would incur high spectral accelerations on a building, (see Figure 1.1). These seismic forces result into high internal forces and stresses on a structure, and hence uneconomical sections are necessary in order for the demand not to exceed the capacity. This problem could only be overcome by designing the building respond nonlinearly in the event of a major In that case, the inelastic design spectrum in Figure 1.1 is used to determine the seismic forces that should be acted on the building for analysis and design of the building. By using these reduced seismic forces, engineers are allowed to simplify the analysis stage by assuming linear elastic material response in load carrying members, while the reality is much different. Actually, imposing a structure to go into nonlinear phase requires solid understanding on its response in the event of seismic excitation, i.e. not only monotonic but cyclic behavior of members become critical. By reducing the level of seismic forces, more economical sections are obtained in practice, but the deformation capacity of the members should be such that those forces are maintained in a ductile fashion during vibrations, i.e. the input earthquake energy should be dissipated by the structural load carrying members.

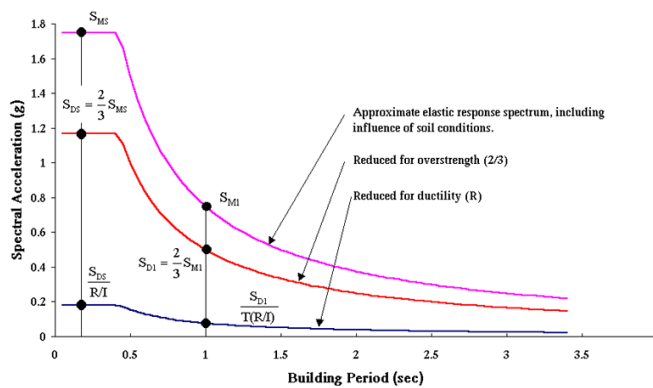


**Figure 1.1: Elastic and Inelastic Design Spectrums**

Regarding the concerns mentioned above, moment resisting steel frames (MRSF) had been considered to be ideal as far as the dissipation of seismic loads are concerned. Besides, structural steel which is inherently ductile, in addition to its other advantages such as rapid erection, high strength and reliability, is a very suitable material for this type of this design, as well. However, due to non-monolithic nature of steel structures, the behavior of connections should be carefully studied. In practice, there are two idealized assumptions on the behavior of steel connections: 1) simple (shear) connection, 2) rigid (moment) connection. In the event of a major seismic excitation, the real behavior of steel connections may need to be taken into account, where not only the monotonic but also the cyclic nonlinear response at connections can result into unexpected failures as observed in 1994 Northridge Earthquake (6.7  $M_w$ ) [13], and 1995 Kobe Earthquake [45]. Furthermore, some connections are actually do not fit into the two idealized assumptions mentioned above, where for such connections, their behavior further becomes more critical. These connections are named as partially restrained/fixed or more popularly semi-rigid in literature and in design specifications AISC [8] and Eurocode [18].

It is critical that the structural system response of moment resisting steel frames are thoroughly studied under major seismic excitations, considering the presence of various possibilities of connection nonlinearity, as well as nonlinearities that may

originate from other load carrying members and due to geometric effects. This thesis provides a contribution in this direction. Before objectives and scope of the thesis are outlined, background on moment resisting frames and simplified models for connections will be presented, and then past studies related to the system investigations on moment resisting steel frames with the inclusion of connection behavior will be documented.

## **1.2 Moment Resisting Steel Frames**

Moment resisting steel frames offer a practical load carrying system against seismic excitations (Figure 1.2). Owing to their flexible nature these frames go well into nonlinear range. Thus, the stiffness and displacement demands should be carefully studied for these structures. Due to high induced lateral displacements, the ductility capacity of each component of MRSF should safely meet the demand. In this regard, the cyclic behavior of beam-column connections become very critical, and the steel connections in MRSF should provide sufficient ductility at the joint region in the event of a major earthquake.

As mentioned before, the idealized behaviors of simple or rigid connections could render a structural analysis model be inapt at reflecting the real behavior. Rigid connections prevents relative rotation between the joining beam and column, whereas pinned connection provides no restraint in rotation and does not transfer any moment. The prevalence of this idealization stems from its simplicity and being easy to use. The welded connections are typically assumed to be fully fixed; whereas connections with bolts mostly fall in a category between the fully rigid and the pinned connections, where these are going to be discussed next.

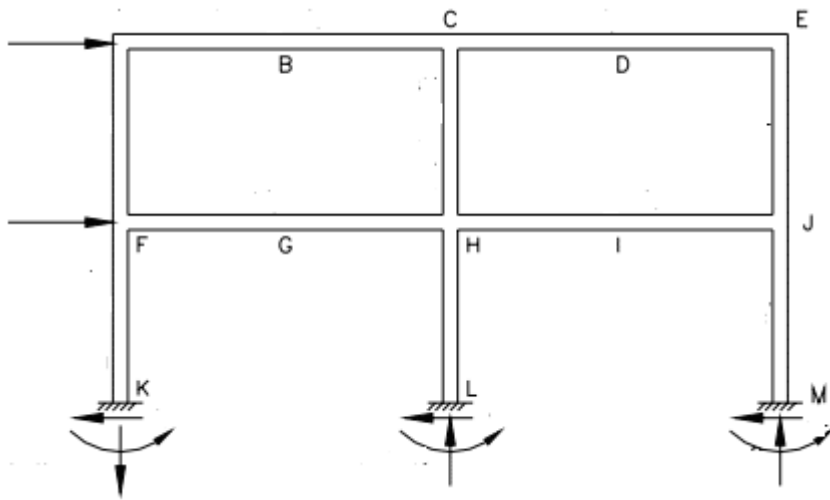


**Figure 1.2: Typical Moment Resisting Frame [48]**

### 1.3 Partially Fixed Connections

The common types of partially restrained/fixed (or also called as semi-rigid) connections are listed below.

#### 1.3.1 Single Web-Angle and Single Plate Connections

Single web-angle connection (Figure 1.3) is built by utilizing an angle that could either be welded or bolted to both column and beam. By the same token, for the single plate connections (Figure 1.4) plate is used instead of an angle, but the plate is welded to column which makes the connection stronger than the web-angle connection. Both of these are the least strong connections among all.

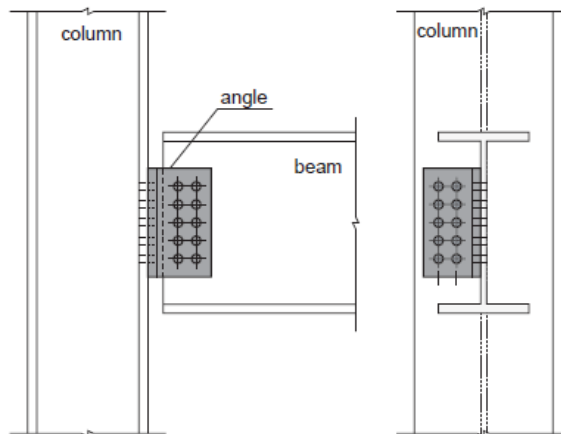


**Figure 1.3: Single Web-Angle connection [48]**

Single plate connection is shown on Figure 1.4.

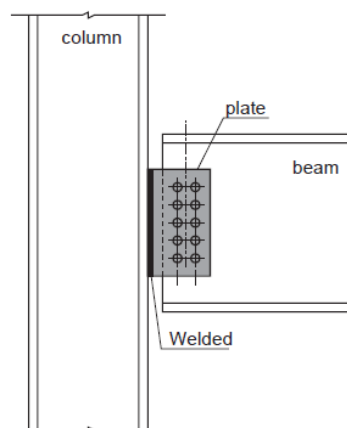


**Figure 1.4: Single Plate connection [48]**

### 1.3.2 Double Web-Angle Connections

In the connection shown in Figure 1.5, both sides of the beam's web are connected to columns and this enhances the moment capacity and the flexural stiffness of the joint.

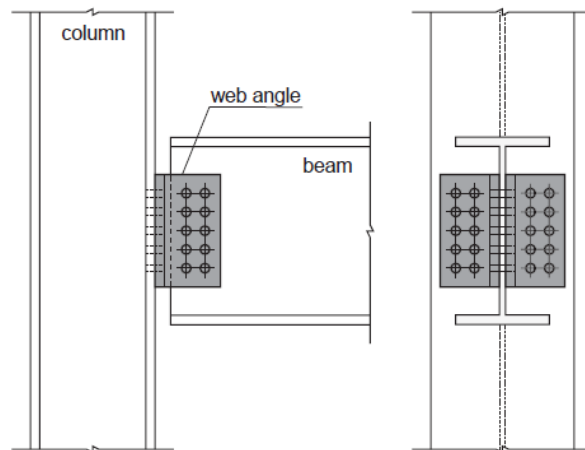


**Figure 1.5: Double Web-Angle [48]**

### 1.3.3 Top and Seat Angle Connections with Double Web Angle

Four pieces of angles are employed for this type of connection, where two of them are attached to flanges as seen in Figure 1.6. Double web angle is introduced so as to reinforce restraint between the top and seat angle connections.

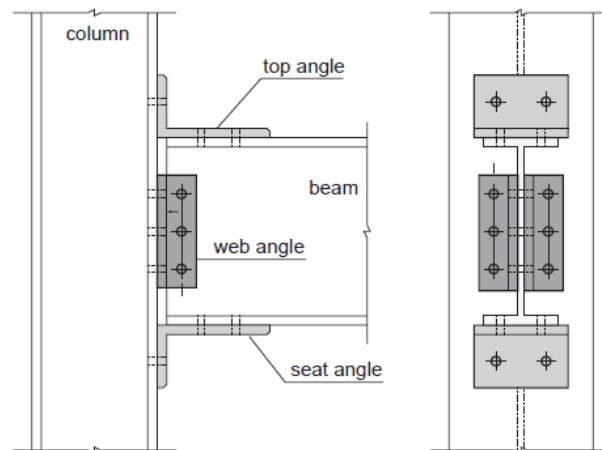


**Figure 1.6: Top and Seat-Angle connection with a Double Web-Angle [48]**

### 1.3.4 Extended End – Plate Connections and Flush End-Plate Connections

The end plates are welded on the beam-side and bolted at the column side in these connections. The end plate is extended on the tension side, which is above the top flange of the beam, , but it can also be extended on the compression side as shown in Figure 1.7. The end plates enhance the moment capacity of the connection and respond to the cyclic loading and moment reversals that could occur due to ground motions. Since the behavior of this connection depends mostly on the stiffness of the column on the joint side, stiffeners of the column flanges are employed near the connection and restrains the flexural deformation.

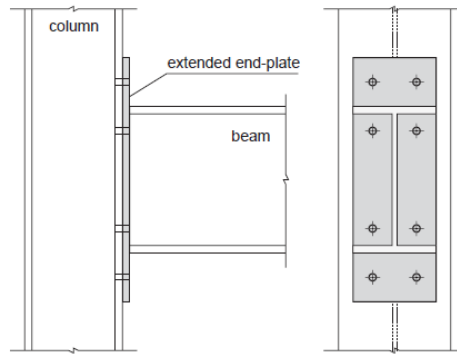


**Figure 1.7: Extended End-Plate connection [48]**

Flush end-plate connection is shown in Figure 1.8. This is not as strong as the extended connections.

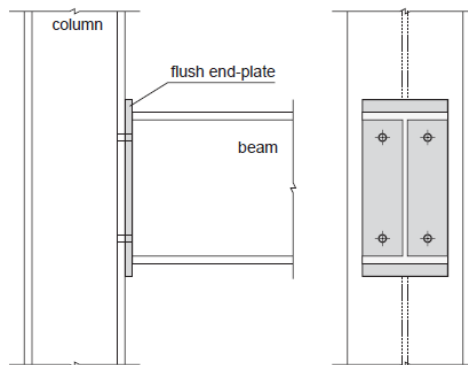


**Figure 1.8: Flush End-Plate Connection [48]**

**1.3.5 Header Plate Connections**

This type of connection is constructed with a plate that is smaller than the beam depth (Figure 1.9). This type of connection is used where moment transfer is abstained and shear transfer is assured.

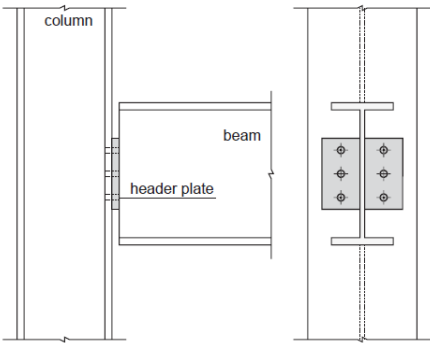


**Figure 1.9: Header Plate Connection [48]**

Figure 1.10 compares the overall moment versus rotation behavior of above connections are presented under monotonic loading. It is evident that these connections can not be idealized as neither rigid nor simple.

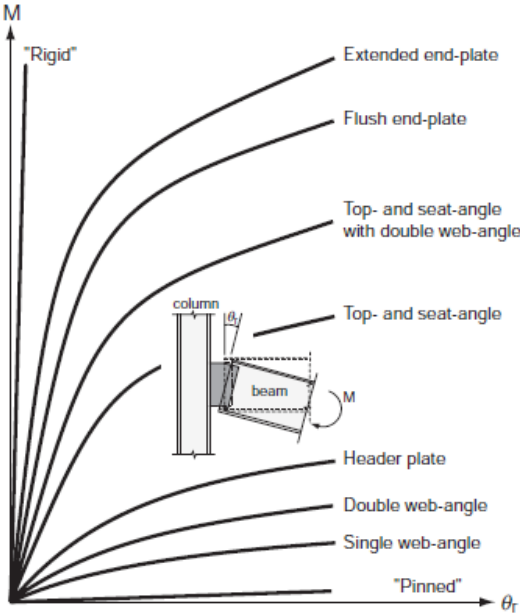


**Figure 1.10: Moment Rotation Curves of The Typical Connections [48]**

After this introduction on moment resisting steel frames and steel connections, literature survey is provided with regards to the analysis and modeling of steel framed structures, taking into account steel connection response.

## **1.4 Literature Survey**

Past studies on models proposed for beam-column steel connections are presented first, and then studies that incorporated the partially fixed behavior of connections in steel frames are given.

### **1.4.1 Proposed models for moment-rotation behavior of beam-column connections**

Krishnamurty et al.[27], Patel and Chen [35], Driscoll [15], and Kukreti et al.[28] carried out detailed finite element analysis to model real behavior of partially restrained connections. However, even creating the geometrical model of a single connection in detail is laborious and its analysis requires too much time, resulting into a nonsuitable modeling approach for structural system analysis. Therefore, researchers diverted their focus to simplified models generated mostly through experiments either through curve fitting or by the use of some theoretical/mechanics-based models. The behavior of connections in literature is thus mostly represented with simplified moment-rotation type models as discussed in [5], [9] and [15]. While this provides practical modeling strategy for beam-column connections, this also requires prediction of the moment-rotation response through curve-fitting from experimental data [18] mostly done under monotonic loading, such as polynomial model or some theoretical models with limitations such as power model [19]. However, extension of these models to cyclic behavior is not straightforward at all. A detailed discussion of these alternatives was presented in a recent study [15].

In vibration or buckling analysis of structures taking into account connection stiffness, the use of linear moment-rotation curves can be utilized, where only the initial stiffness is needed. This model can also be used when very small rotations are present or assuming connection nonlinearity is not an issue to worry about.

The most commonly used nonlinear model for steel connections are the Frye-Morris Polynomial Model [21], Modified Exponential Model [26] and Three-Parameter Power Model [40]. These will be explained below for the sake of completeness.

#### **1.4.1.1 Frey-Morris Polynomial Model**

The formulation of this model is simple, and this makes the model the most commonly used one among all the models for describing the monotonic nonlinear behavior of steel connections. The formulation is as below:

$$\theta_r = C1(KM)^1 + C2(KM)^3 + C3(KM)^5 \quad (1.1)$$

where  $C1$ ,  $C2$  and  $C3$  are the curve-fitting constants and are given in Table 1.1.

The main drawback of this formulation is that the tangent connection stiffness might become negative at some value of connection moment  $M$  which is not physically acceptable. Besides the negative stiffness would cause numerical difficulty in the analysis.

**Table 1.1: Curve-Fitting Constants and Standardization Constants for Frye-Morris Polynomial Model (all size parameters are in centimeters) [48]**

Connection Types	Curve-Fitting Constants	Standardization Constants
<b>Single web-angle connection</b>	C1=1.67x10 <sup>0</sup> C2=8.56x10 <sup>-2</sup> C3=1.35x10 <sup>-3</sup>	K=d <sub>a</sub> <sup>-2.4</sup> t <sub>a</sub> <sup>-1.81</sup> g <sup>0.15</sup>
<b>Double web-angle connection</b>	C1=1.43x10 <sup>-1</sup> C2=6.79x10 <sup>1</sup> C3=4.09x10 <sup>5</sup>	K=d <sub>a</sub> <sup>-2.4</sup> t <sub>a</sub> <sup>-1.81</sup> g <sup>0.15</sup>
<b>Top-and seat-angle with double web-angle connection</b>	C1=1.50x10 <sup>-3</sup> C2=5.60x10 <sup>-3</sup> C3=4.35x10 <sup>-3</sup>	K=d <sup>-1.5</sup> t <sup>-0.5</sup> t <sub>c</sub> <sup>-0.415</sup> l <sub>a</sub> <sup>-0.7</sup> d <sub>b</sub> <sup>-1.1</sup>
<b>Top-and seat-angle without double web-angle connection</b>	C1=2.59x10 <sup>-1</sup> C2=2.88x10 <sup>3</sup> C3=3.31x10 <sup>4</sup>	K=d <sup>-1.5</sup> t <sup>-0.5</sup> t <sub>c</sub> <sup>-0.415</sup> l <sub>a</sub> <sup>-0.7</sup> d <sub>b</sub> <sup>-1.1</sup>
<b>End-plate connection with column stiffeners</b>	C1=1.67x10 <sup>0</sup> C2=8.56x10 <sup>-2</sup> C3=1.35x10 <sup>-3</sup>	K=d <sub>a</sub> <sup>-2.4</sup> t <sub>a</sub> <sup>-1.81</sup> g <sup>0.15</sup>
<b>T-stub connection</b>	C1=1.67x10 <sup>0</sup> C2=8.56x10 <sup>-2</sup> C3=1.35x10 <sup>-3</sup>	K=d <sub>a</sub> <sup>-2.4</sup> t <sub>a</sub> <sup>-1.81</sup> g <sup>0.15</sup>
<b>Header-plate connection</b>	C1=1.67x10 <sup>0</sup> C2=8.56x10 <sup>-2</sup> C3=1.35x10 <sup>-3</sup>	K=d <sub>a</sub> <sup>-2.4</sup> t <sub>a</sub> <sup>-1.81</sup> g <sup>0.15</sup>

#### 1.4.1.2 Modified Exponential Model

Linear components were inserted by Kishi et al [26] into the exponential model presented by Lui and Chen [17]. The form of the model is as the following:

$$M = M_o + \sum_{j=1}^m C_j (1 - \exp(-\frac{|\theta_r|}{2j\alpha})) + \sum_{k=1}^{mn} D_k (|\theta_r| - |\theta_k|) H (|\theta_r| - |\theta_k|) \quad (1.2)$$

Where  $M_o$ ,  $\alpha$ ,  $C_j$ ,  $D_k$ ,  $\theta_k$  are the initial connection moment, scaling factor, curve fitting constants and the starting rotation for the k-th linear components respectively.

In order to obtain the instantaneous stiffness  $R_k$  the equation below is used.

$$R_k = R_{kt} = \frac{dM}{d|\theta_r|} \Big|_{@|\theta_r|} = \sum_{j=1}^{nm} \frac{C_j}{2j\alpha} \exp\left(-\frac{|\theta_r|}{2j\alpha}\right) + \sum_{k=1}^n D_k H(|\theta_r| - |\theta_k|) \quad (1.3)$$

### 1.4.1.3 Three-Parameter Power Model

The power model is mostly attributed to the work by Krishnamurty et al [27]. Later on, the original model was used in the following simplified form, named as three-parameter power model:

$$M = \frac{R_{ki}\theta_r}{\left(1 + \left(\frac{\theta_r}{\theta_0}\right)^n\right)^{1/n}} \quad (1.4)$$

The shape parameter  $n$  is obtained using the method of least squares for the differences between the predicted and the test data.

$$R_k = \frac{dM}{d\theta_r} = \frac{R_{ki}}{\left(1 + \left(\frac{\theta_r}{\theta_0}\right)^n\right)^{(n+1)/n}} \quad (1.5)$$

$R_k$  is the initial stiffness of the connection.  $M_u$  is the ultimate moment capacity.

$$\theta_r = \frac{M}{R_{ki} \left(1 - \left(\frac{M}{M_u}\right)^n\right)^{1/n}} \quad (1.6)$$

Tangent stiffness and the relative rotation are determined from the the equation above in a direct manner.

#### **1.4.1.4 Cyclic moment-rotation models for steel connections**

Description of cyclic behavior of connections with the use of nonlinear models with continuous functions is not very practical as outlined by Saritas and Koseoglu [5]. In this regard, the efforts undertaken by Sekulovic and Salatic [44], Valipour and Bradford [46] can be cited, where these models are similar to the above mentioned monotonic models, but consider the presence of cyclic response as an added feature. However, these models did not consider the effects of stiffness and strength degradation, as well as pinching effects in the description of moment-rotation behavior of the connections. The model proposed by Nogueiro [33] included many of the important features for capturing the cyclic behavior of connections. The nonlinear cyclic definitions of these models are actually adopted from uniaxial stress-strain models proposed by Ramberg and Osgood [38], Richard and Abbott [41].

Instead of using nonlinear models with continuous functions, it is actually more practical to use multi-linear or piecewise linear models. One of the simplest such model can be adopted from uniaxial plasticity model with kinematic hardening, where this was used by Abolmaali [6]. In order to increase more features, at least trilinear response with possibility of strength and stiffness degradation and pinching effects should be used. Such a model was used in a previous study by Karakas was also proposed by Saritas and Koseoglu [5].

#### **1.4.2 Studies on the effect of partially restrained connections on steel frames**

In here some of the most significant and relevant studies on the investigation of the system response of steel framed structures including nonlinearity at connection regions are outlined.

Chen and Lui [17] undertook arguably the pioneering work on this subject. For their model, beam/column element approach was preferred over detailed finite element analysis with solid elements. In their model, axial force and bending moment

interaction of member capacities were taken into account. In order to capture large displacements lagrangian coordination is adopted where the disturbed shape is regarded as the reference. Moment-rotation behavior of the connections were modeled through the use of power model. Incremental load control Newton-Raphson was selected in which a small load increment was imposed than iterations were done on the displacements so that the load difference would fall in a limit. Three models were tested in order to capture the effect of the partially restrained (PR) connections. First, a snap-through problem with geometric non-linearity was considered, where upto the snap-through phase no difference was noted but after the snap-through due to excessive deformation the stiffness of the connection was almost null which yielded considerable difference on the behavior compared to the model with rigid connections. The second and third examples considered a portal frame and a four-story single bay frame. Overall, it was emphasized that the PR nature of the connections should not be omitted in the analysis of steel structures.

Lui and Chen [\[16\]](#) had published another study on the following year. Two examples were carried out to grasp the behavior better. First, sway restrained pin based portal frame was used. Three types of connections were employed, i.e. weak, strong and rigid. It was found that the load carrying capacity of a portal frame was not influenced by the type of connection, and the weaker connections delay the plastification of columns. Besides, it was demonstrated that, for the sake of simplicity, connections that are stronger than beam and columns could be identified as rigid. It was noted that weak connections render instability whereas strong connections display beam mechanism. Overall, it was concluded that the connections performs linear when unloading but it acts nonlinearly during loading, and furthermore flexible connections deform more.

Elnashai and Elghazouli [\[4\]](#), in 1994, published a paper raising that PR connections poses stability problems, whereas, at the same time fully rigid (FR) connections (assumed as welded connection) failed to sustain integrity under severe ground motions. The benefit of PR connections for yielding longer period, thus, decreasing the inertial force was indicated. In order to investigate the behavior with PR connections with respect to rigid case, five two-story single bay frames were tested, as

well as modeled by ADAPTIC program [24]. Frames with PR connections (semi-rigid frames) showed sufficient performance under these experiments and proved to be stable and ductile, and the finite element program was able to capture the response in an acceptable range. An analytical study was also undertaken, and it was concluded that in the absence of stability problems, semi-rigid frames perform well against ground motions, thanks to their ductile nature, although their ultimate load capacity may be inferior to rigid frames. It has been emphasized that the type of connection might effect the location of the plastic hinges. Additionally, the even more need for the designation of point of contra-flexure and plastic hinges for the optimum design was emphasized.

Gerstle [29] made use of different semi-rigid connection models in order to investigate the effects of rotational flexibility of beam-column connections on the behavior of unbraced steel frames. The results of the analyses was compared with the tests and a practical design approach was developed.

Maison and Kasai [11], studied the low-rise and mid-rise SAC buildings [39] with PR connections that were analyzed under both push-over and nonlinear time history analyses for which 20 ground motion data with 10% and 2% of probability of exceedance for 50 years was used. The natural periods were compared. Base shear/weight versus roof drift ratio graphs were generated. The effect of PR connections on these structures was studied by varying the stiffness, yield and hardening moment of the connection. It was concluded that the performance of the frames with PR connections is similar to that of the frames with the rigid connections. Energy dissipation of special moment resisting frames with semi-rigid connections, and provision of redundancy are accentuated, and the utilization of semi-rigid connections were encouraged in that study. It was reached that the natural period of the frames were not primarily depending on the type of the semi-rigid connections but on the beams and columns. It was also concluded in the study that the reduction of the stiffness of the connection have less significance compared to the hardening and the yield moment of the connection.

Balendra and Huang [12] studied the behavior of braced frames and the frames with semi-rigid connections. Push-over analysis was conducted. It was concluded that the inclusion of the semi-rigid connections in the frames caused about 50% decrease in the overstrength of the frame, whereas the ductility factor is increased by 25%.

Related with the dynamic behavior of the special moment resisting frames (SMRF), Akshay and Helmut [7] carried out a detailed study in which the parameters were the height of the building and the seismic zone of the region. Both push-over analysis and nonlinear time history analysis were carried out. In 2011, Aksoylar et al [32] have published a study merely for the low-rise SMRF with PR connections so as to derive alternative and reliable framing systems. Several parameters, i.e. span lengths, connections strengths, pinching, were taken into account. Both push-over and nonlinear time history analysis were conducted. For the nonlinear time history analysis 25 ground motion records were utilized. All the 26 model did perform sufficient for both type of analysis.

Recently, Karakas [50] studied the effect of multiple parameters of the semi-rigid connections, that are the stiffness, yield and ultimate moment capacity and the presence of strength loss and pinching, on the hysteretic behavior of the low-rise special moment resisting steel frames. Both push-over and nonlinear time history analysis were conducted for the lower bound and the upper bound cases of the structures, where the structures were taken from Lee and Foutch [25]. Interstory drift ratios (IDR) were recorded and checked with respect to the performance levels stated in FEMA 356. It was observed that even the 84<sup>th</sup> percentile of the IDR did not exceed the limit of collapse prevention, i.e. 5%, for the upper bound design. It was concluded that the stiffness of the connection was the mere factor of the connection to effect the natural period of the building. The pinching did not cause drastic change on the behavior of the frame.

## 1.5 Objectives and Scope

Moment resisting steel frames (MRSF) are considered to provide an ideal load resisting system and energy dissipation capacity in the event of major seismic excitations. However, there are certain idealizations considered in the analysis and design stages of these framing systems, and these idealizations contain some risks and these should be thoroughly studied. At the 1994 Northridge earthquake ( $M_w$  6.7), 150 steel MRF buildings experienced beam-to-column fractures. The prevalent failure was at the weld of the bottom flange to the column. This case disturbed the decades' conviction that the frames with welded joints could provide the ductility demand and strength level required for the energy dissipation. However, the fractures at the connection resulted in sudden loss in the strength and stiffness and hampered the expected ductile behavior. Following this failure, SAC Steel project [25] was organized focusing on the steel moment resisting frame behavior. In this thesis, mid-rise and high-rise buildings considered in SAC Project [25] will be studied specifically focusing on the level of connection nonlinearity that may be faced in real case, and this effort is going to complete a prior effort undertaken by Karakas [50] for the low-rise frames.

Most of the investigations on MRSF were carried out on low-rise or even portal frames in the literature. This thesis will provide more in depth parametric study on the mid-rise and high-rise buildings which might accentuate the significance of the parameters considered for defining connection nonlinearity, and thus also provide a correlation with the responses observed in low-rise buildings in the study Karakas [50]. It is expected that the higher mode effects and stability problems might pose further risks as the height of the building increases.

In order to assess the performance level of the considered mid-rise and high-rise buildings, push-over analysis will also be carried out. Most accurate assessment of the nonlinear behavior of the structures will be obtained through time history analysis by the use of scaled ground motions. Within the scope of the study, the ability of energy dissipation characteristics of the connections will be sought, as well.

The organization of the thesis is as follows:

In Chapter 2, the selected structural analysis program along with the employed models will be presented. For the parametric study, the considered mid-rise and high-rise buildings plan and elevation view, as well as their material and geometric properties are also provided in this chapter.

In Chapter 3, the push-over and the nonlinear time history analysis tools will be discussed, and the selected ground motions will be presented.

In Chapter 4, the results obtained from push-over and time history analyses will be presented with discussions.

Finally, conclusions from this thesis will be given in Chapter 5.

## CHAPTER 2

### ANALYZED BUILDINGS

In this chapter, the moment resisting steel frames used for the parametric study undertaken in this thesis are presented. For these frames, inclusion of partial fixity at beam-column connections is attained through a moment-rotation type cyclic model. The parameters employed in the steel connections are outlined at the end of the chapter.

#### 2.1 Description of the Buildings

Aftermath of the 1994 Northridge Earthquake, the SAC Project [\[25\]](#) designed three buildings named as Post-Northridge buildings in order to comply with the 1997 NEHRP and AISC provisions [\[29\]](#). The three buildings have following story heights:

- 3 story (Low-Rise)
- 9 story (Mid-Rise)
- 20 story (High-Rise)

In a previous study, Karakas [\[50\]](#) studied the low-rise Post-Northridge SAC Buildings in detail. This thesis is interested in the influence of connection nonlinearity on the overall performance of the mid-rise and high-rise Post-Northridge SAC Buildings. Thus, in here only the mid-rise and high-rise SAC buildings will be presented.

The material used for the steel is the same for all buildings, namely A572 Grade 50, and the detailed material properties are listed below:

- Yield stress  $F_y = 345 \text{ MPa}$
- Elasticity modulus  $E = 200 \text{ GPa}$
- Shear modulus  $G = 77 \text{ GPa}$
- Poisson's ratio value of 0.3.
- Strain hardening value of 0.03.

### 2.1.1 Mid-Rise (9-Story) Building

The 9-story building has span length of 30 ft (914 cm) in both directions on plan view (Figure 2.1). The elevation view of the building is shown in Figure 2.2. The basement story height is 12 ft (366 cm), the first story height is 18 ft (549 cm) and the rest of the stories have 13 ft (396 cm) height. As can be seen from the plan view, the buildings were designed with perimeter moment resisting frames that carry the lateral load, and the intermediate frames were designed to carry only gravity loads.

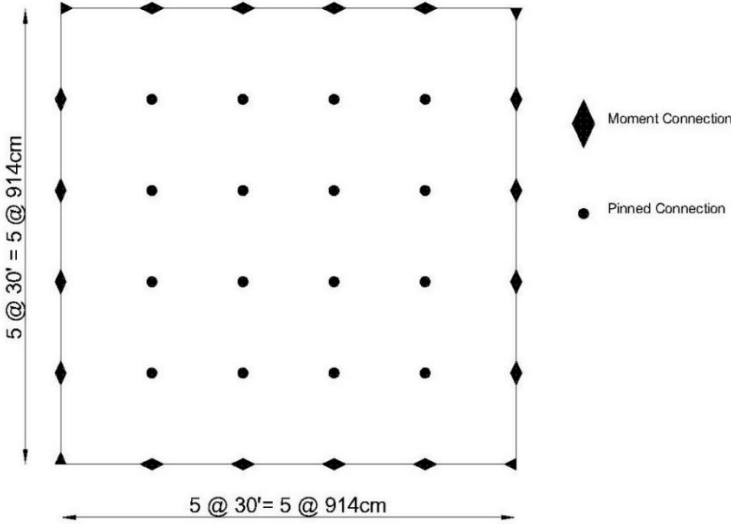


**Figure 2.1: Plan View of the 9-Story Building**

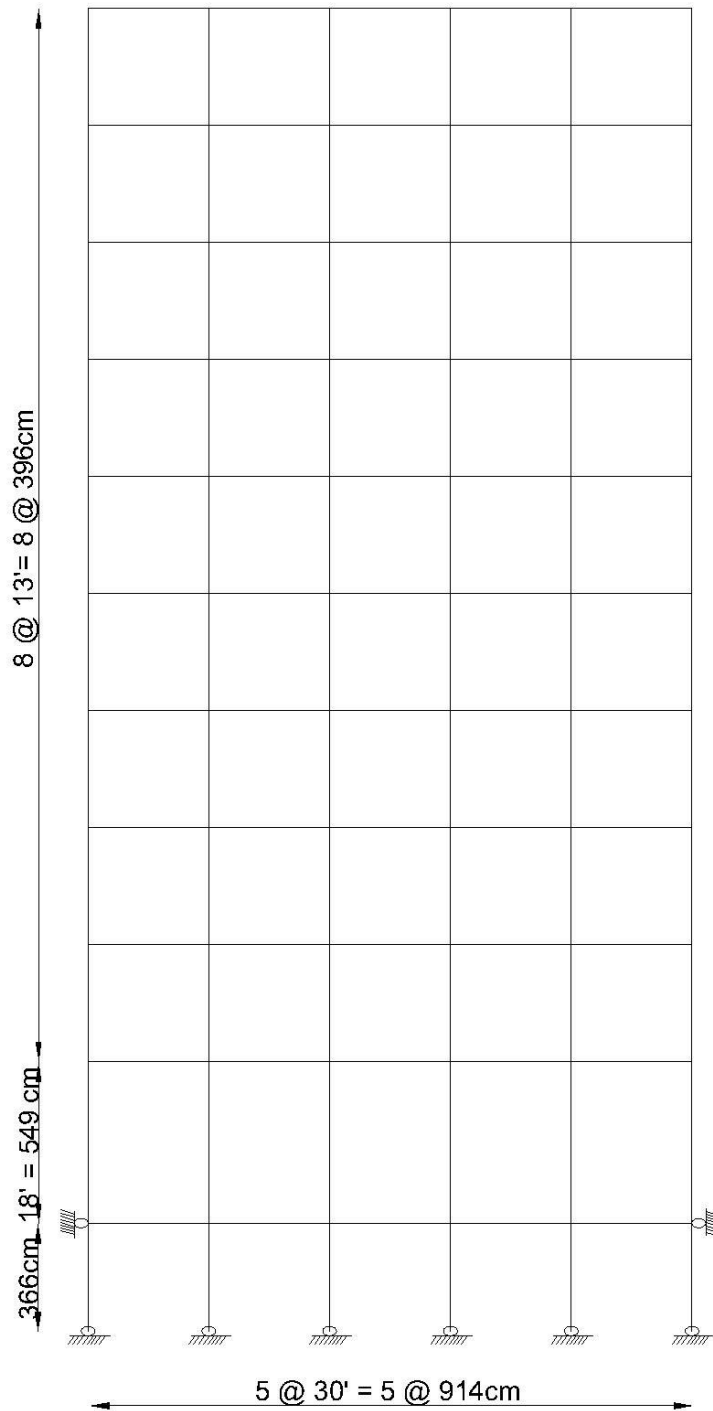


**Figure 2.2: Elevation View of the 9-Story Building**

### 2.1.1.1 Floor Masses for the 9-Story Buildings

In-depth loading and mass configurations, that are the live and the service loads, could be found at the SAC/BD-00/25 report. The overall mass representing all the loads for each level are as follows:

- Level 1 = 1007 tons (69 kips – sec<sup>2</sup>/ft)
- Level 2 – 8 = 989 tons (67.8 kips – sec<sup>2</sup>/ft)
- Level 9 = 1067 tons (73.1 kips – sec<sup>2</sup>/ft)

No mass is assigned at the ground level since that floor's lateral movement is restricted and no inertial force will be induced due to ground motion.

### 2.1.1.2 The Frame Configuration for the 9-Story Building

The Post-Northridge buildings were originally presented in SAC Project report [\[25\]](#) and the buildings were designed considering the use of four different W column dimensions (W14, W24, W30 and W36 columns). For each choice of W column dimension (let's say W14), the column depth was kept constant throughout the whole height of a building (i.e. W14 column dimension was used for all columns), and the rest of the cross-section parameters were adjusted accordingly from that group of W column dimension (e.g. see Table 2.1 for the chosen W14 column sections for the internal and external columns for 9-story building).

Later on, Lee and Foutch [\[25\]](#) redesigned the low-rise and mid-rise buildings in order to provide variation on the periods for each choice of W column dimension. In their report, they provided an upper bound (UB) and lower bound (LB) versions of the buildings, thus increasing the number of buildings for low-rise and mid-rise to 8 different cases. The upper bound design yields conservative results and provides a stiffer version of the designed structure. The lower bound design was obtained considering the base shear resulting considering the drift check according to the

allowances of 1997 NEHRP, and resulting in a flexible version of the designed structure. The high-rise building had only one design due to the increased height of the building.

In this thesis for the mid-rise buildings, LB designed version of W14 column configuration and UB designed version of W36 column configuration are chosen for the parametric study, where this selection provides the most flexible and stiff designed versions of the mid-rise buildings, respectively. This selection will allow us to study the influence of structure stiffness on the overall response of the structure, especially within the context of the influence of connection nonlinearity. The column and the beam sizes and their configurations are presented below for the selected 9-story buildings.

**Table 2.1: Column and Beam Geometric Properties for W14 LB design of 9-Story Building**

Story/Floor	W-Sections		
	Columns		Girder
	Exterior	Interior	
-1/1	w14x500	w14x550	w36x150
1/2	w14x500	w14x550	w36x150
2/3*	w14x455	w14x550	w36x150
3/4	w14x455	w14x550	w33x141
4/5*	w14x398	w14x455	w33x141
5/6	w14x398	w14x455	w33x141
6/7*	w14x283	w14x398	w30x116
7/8	w14x283	w14x398	w30x116
8/9*	w14x257	w14x283	w27x94
9/Roof	w14x257	w14x283	w21x62

**Table 2.2: Geometric Dimensions of Column Sections for W14 LB Design of 9-Story Building**

Section	Depth	Width	Web Thickness	Flange Thickness	Sectional Area
	d (mm)	b <sub>f</sub> (mm)	t <sub>w</sub> (mm)	t <sub>f</sub> (mm)	A (cm <sup>2</sup> )
W 14 x 500	498	432	56	89	948
W 14 x 455	483	428	51	82	865
W 14 x 398	465	421	45	72	755
W 14 x 283	425	409	33	53	537
W 14 x 257	416	406	30	48	488
W 14 x 550	514	437	60	97	1045

**Table 2.3: Geometric Dimensions of Girder (Beam) Sections for W14 LB Design of 9-Story Building**

Section	Depth	Width	Web Thickness	Flange Thickness	Sectional Area
	d (mm)	b <sub>f</sub> (mm)	t <sub>w</sub> (mm)	t <sub>f</sub> (mm)	A (cm <sup>2</sup> )
W 36 x 150	911	304	16	24	285
W 33 x 141	846	293	15	24	268
W 30 x 116	762	267	14	22	221
W 27 x 94	684	254	12	19	179
W 21 x 62	533	209	10	16	118

**Table 2.4: Column and Beam Geometric Properties for W36 UB Design of 9-Story Building**

Story/Floor	W-Sections		
	Columns		Girder
	Exterior	Interior	
-1/1	W36x210	W36x280	W36x182
1/2	W36x210	W36x280	W36x182
2/3*	W36x210	W36x256	W36x150
3/4	W36x210	W36x256	W36x150
4/5*	W36x182	W36x210	W36x150
5/6	W36x182	W36x210	W36x150
6/7*	W36x150	W36x182	W33x118
7/8	W36x150	W36x182	W33x118
8/9*	W36x135	W36x150	W27x94
9/Roof	W36x135	W36x150	W21x62

**Table 2.5: Geometric Dimensions of Column Sections for  
W36 UB design of 9-Story Building**

Section	Depth	Width	Web Thickness	Flange Thickness	Sectional Area
	d (mm)	b <sub>f</sub> (mm)	t <sub>w</sub> (mm)	t <sub>f</sub> (mm)	A (cm <sup>2</sup> )
W 36 x 210	932	309	21	35	399
W 36 x 182	923	307	18	30	346
W 36 x 150	911	304	16	24	285
W 36 x 135	903	304	15	20	256
W 36 x 280	928	422	22	40	532
W 36 x 256	951	310	24	44	486

**Table 2.6: Beam Sizes for the W36 UB Design of 9-Story Building**

Section	Depth	Width	Web Thickness	Flange Thickness	Sectional Area
	d (mm)	b <sub>f</sub> (mm)	t <sub>w</sub> (mm)	t <sub>f</sub> (mm)	A (cm <sup>2</sup> )
W 36 x 182	923	307	18	30	346
W 36 x 150	911	304	16	24	285
W 33 x 118	835	292	14	19	224
W 27 x 94	684	254	12	19	179
W 21 x 62	533	209	10	16	118

### 2.1.2 High-Rise (20-Story) Building

The 20-story building has span length of 20 ft (609cm) in both directions on plan shown in Figure 2.4. The elevation of the structure is shown in Figure 2.3. The height of the two basement stories are 12 ft (366 cm), the first story height is 18 ft (549 cm) and the rest of the stories have 13 ft (396 cm) height. The building is designed with perimeter moment resisting frames, and the intermediate frames were designed to carry only gravity loads. Different from the nine story building, this one has two basement floors, which are again restrained from lateral movement by the presence of perimeter walls, besides, the corner columns experience bi-axial bending even under the gravity loading condition.

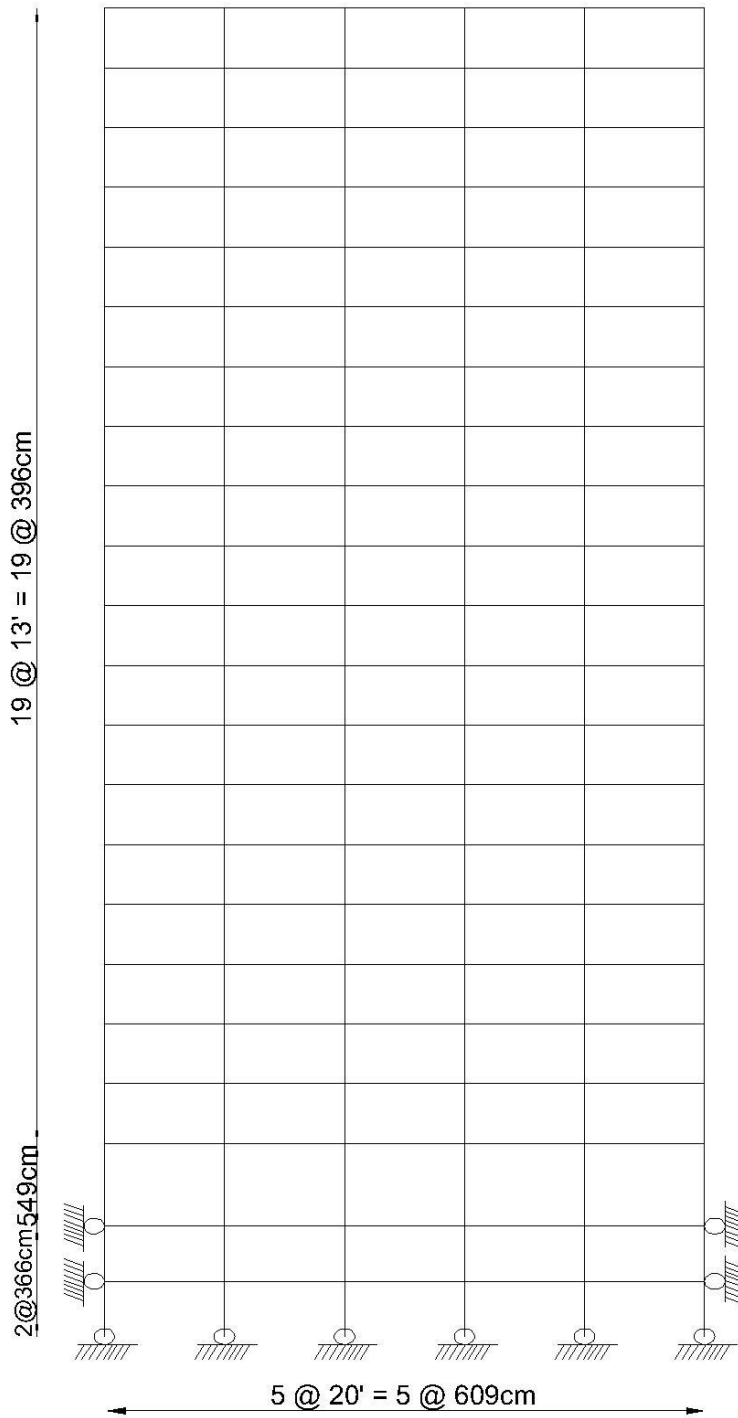


**Figure 2.3: Elevation View of 20-Story Building**

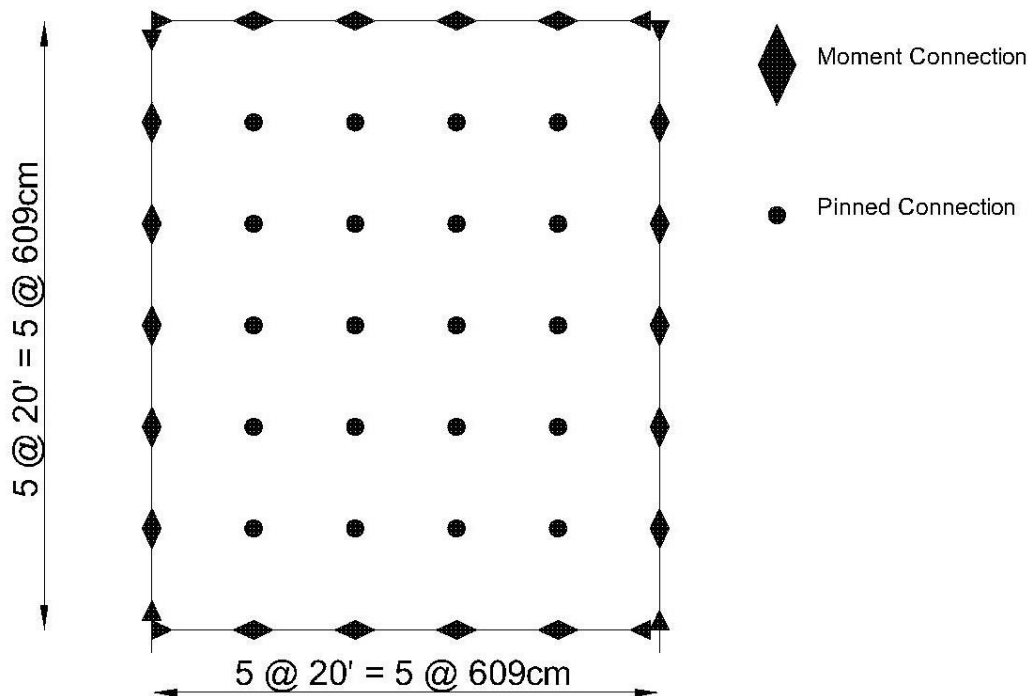


**Figure 2.4: Plan View of the 20-Story Building**

### 2.1.2.1 Floor Masses for the 20-Story Buildings

The overall mass at each floor level are given in SAC/BD-00/25 report, and they are:

- Level 1 = 563 tons (38.6 kips – sec<sup>2</sup>/ft)
- Level 2 – 19 = 550 tons (37.7 kips – sec<sup>2</sup>/ft)
- Level 20 = 592 tons (40.6 kips – sec<sup>2</sup>/ t)

No mass is assigned at the ground level and the basement since that floor's lateral movement is restricted and no inertial force will be induced due to ground motion.

### 2.1.1.2 The Frame Configuration for the 20-Story Building

The 20-story building in the SAC Project report [25] does not have upper/lower bound design due to increased height. There are 4 types of buildings in the report for this height with respect to the column size selection (W14, W24, W30 and W36 columns). In this thesis, the model with W14 dimensions is used. However, different from the 9-story building, hollow square sections are used at the corner columns. The column and the beam sizes and their configurations are presented below.

**Table 2.7: Column and Beam Geometric Properties for W14 Design of 20-Story Building**

Story/Floor	W-Sections		
	Columns		Girder
	Exterior	Interior	
-2/-1	15x15x2.0	W14x808	W14x22
-1/1	15x15x2.0	W14x808	W33x130
1/2	15x15x2.0	W14x808	W33x130
2/3	15x15x2.0	W14x730	W33x118
3/4	15x15x2.0	W14x730	W33x118
4/5	15x15x2.0	W14x730	W36x135
5/6	15x15x1.25	W14x665	W36x135
6/7	15x15x1.25	W14x665	W36x135
7/8	15x15x1.25	W14x665	W36x135
8/9	15x15x1.25	W14x605	W36x135
09/10	15x15x1.25	W14x605	W36x135
10/11	15x15x1.25	W14x605	W36x135
11/12	15x15x1.0	W14x605	W36x135
12/13	15x15x1.0	W14x605	w36x135
13/14	15x15x1.0	W14x605	w33x118
14/15	15x15x1.0	W14x500	W33x118
15/16	15x15x1.0	W14x500	W30x108
16/17	15x15x1.0	W14x500	W30x108
17/18	15x15x0.75	W14x426	W30x108
18/19	15x15x0.75	W14x426	W27x84
19/20	15x15x0.50	W14x370	W24x55
20/Roof	15x15x0.50	W14x370	W18x46

**Table 2.8: Geometric Dimensions of Column Sections for W14 Design of 20-Story Building**

Section	Depth	Width	Web Thickness	Flange Thickness	Sectional Area
	d (mm)	b <sub>f</sub> (mm)	t <sub>w</sub> (mm)	t <sub>f</sub> (mm)	A (cm <sup>2</sup> )
W 14 x 808	579	472	95	130	1529
W 14 x 730	569	454	78	125	1387
W 14 x 665	550	448	72	115	1265
W 14 x 605	531	442	66	106	1148
W 14 x 500	498	432	56	89	948
W 14 x 426	474	424	48	77	806

**Table2.9: Geometric Dimensions of Girder (Beam) Sections for W14 Design of 20-Story Building**

Section	Depth	Width	Web Thickness	Flange Thickness	Sectional Area
	d (mm)	b <sub>f</sub> (mm)	t <sub>w</sub> (mm)	t <sub>f</sub> (mm)	A (cm <sup>2</sup> )
W 14 x 22	349	127	6	9	42
W 18 x 46	459	154	9	15	87
W 24 x 55	599	178	10	13	105
W 27 x 84	678	253	12	16	160
W 36 x 135	903	304	15	20	256
W 33 x 118	835	292	14	19	224
W 33 x 130	840	292	15	22	247
W 30 x 108	758	266	14	19	205

## 2.2 Modeling Procedure

OpenSees [42] structural analysis program is utilized for carrying out both push-over and time history analysis of the considered buildings in this thesis. OpenSees has vast library of nonlinear solution algorithms, element and material libraries in order to carry out nonlinear analysis of framed structures, and has been extensively used in research. In the next subsections, brief description of the models employed from OpenSees will be presented.

### 2.2.1 Frame Element Selection

The frame element types available in OpenSees [42] are presented in Table 2.10. Among these models, force-based beam column element (*forceBeamColumn*) is utilized due to its robust and accurate response for nonlinear structural analysis. In depth discussion of the accuracy of force-based frame elements is available in Saritas and Soydas [43].

In order to take into account the variation of axial load and its effects on the bending moment capacity for the structural members, fiber discretization is considered. Each section is divided into 10 layers along the depth and 5 layers along the web of the I-section, where normal stress-strain variation at each material point is assumed to be obtained through a bilinear material response. Inclusion of shear effects is considered by section aggregator property in OpenSees. Shear stress is assumed to be uncoupled from normal stress, and furthermore, the shear stress is assumed to remain in the elastic range. In order to obtain an accurate representation of the shear effects, a correction coefficient as suggested by Charney [19] and Ozel and Saritas [23] is considered. A similar approach was also undertaken by Karakas [50]. The correction for shear is as follows:

$$A_v = \frac{A}{K}; \quad \text{Where } K = 0.85 + 1.16 \frac{2b_f}{dt_w} \quad (2.1)$$

Where  $A_v$  stands for the effective shear area and the  $A$  and the  $d$  are the area and the depth of the I-section.

**Table 2.10: Beam-Column Elements in OpenSees [42]**

<b>Element Name and Script in OpenSees</b>	<b>Behavior</b>
Elastic Beam Column Element (elasticBeamColum)	Creates an elastic beam column element
Elastic Beam Column Element with Stiffness Modifiers (ModElasticBeam2d)	Creates a structural element with an equivalent combination of one elastic element with stiffness-proportional damping, and two springs at its two ends with no stiffness proportional damping to represent a prismatic section
Elastic Timoshenko Beam Column Element (ElasticTimoshenkoBeam)	an elastic beam-column element that accounts for shear deformations
Beam with Hinges Element (BeamWithHinges)	Structural element which is based on the non-iterative (or iterative) flexibility formulation. The locations and weights of the element integration points are based on so-called plastic hinge integration which allows the user to specify plastic hinge lengths at the element ends.
Displacement-Based Beam-Column Element	Structural element which is based on the displacement formulation, and considers the spread of plasticity along the element.
Force-Based Beam-Column Element (forceBeamColumn)	Creates a structural element, which is based on the iterative force-based formulation. A variety of numerical integration options can be used in the element state determination and encompass both distributed plasticity and plastic hinge integration.

### **2.2.2 Analysis Models and Idealizations**

The SAC Buildings have symmetric plan and their stiffness and mass centroid coincide as can be seen from the plan and elevations views given in prior sections. For these kinds of buildings, torsional irregularity is minimal, thus analysis of the load carrying frames can be carried out in 2D, i.e. in the plane.

Since the elevation views of the buildings are given in prior sections, in here the structural model is drawn only for one story level in Figure 2.5. Each column and girder is modelled through the use of a single force-based element, where five Gauss-Lobatto integration points are considered for tracking the spread of plasticity along each element length. At the stage of idealizing the 3D building as a 2D model, the mass and the gravity loads on the interior columns are acted on a lean-on-column as lumped mass and weight as shown in Figure 2.5. The mass and weight adjacent to the beams in the load carrying frame are calculated from the tributary area shown in the figure and distributed onto the beams. The lean-on-column is connected to the planar moment resisting frame model through the use of axially rigid truss. Furthermore, the lean-on-column itself is also assigned to have axially rigid truss properties, i.e. it has negligible flexural stiffness and axial deformation.

Since moment resisting frame structures can undergo significant lateral displacements, nonlinear geometric effects can become important in the overall response of the structure. For this purpose, corotational transformation available in OpenSees is employed for all vertical elements, and linear transformation is used for the beams.

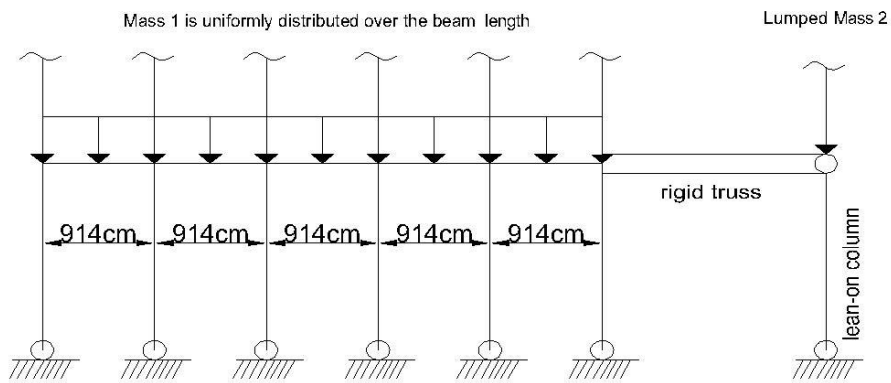
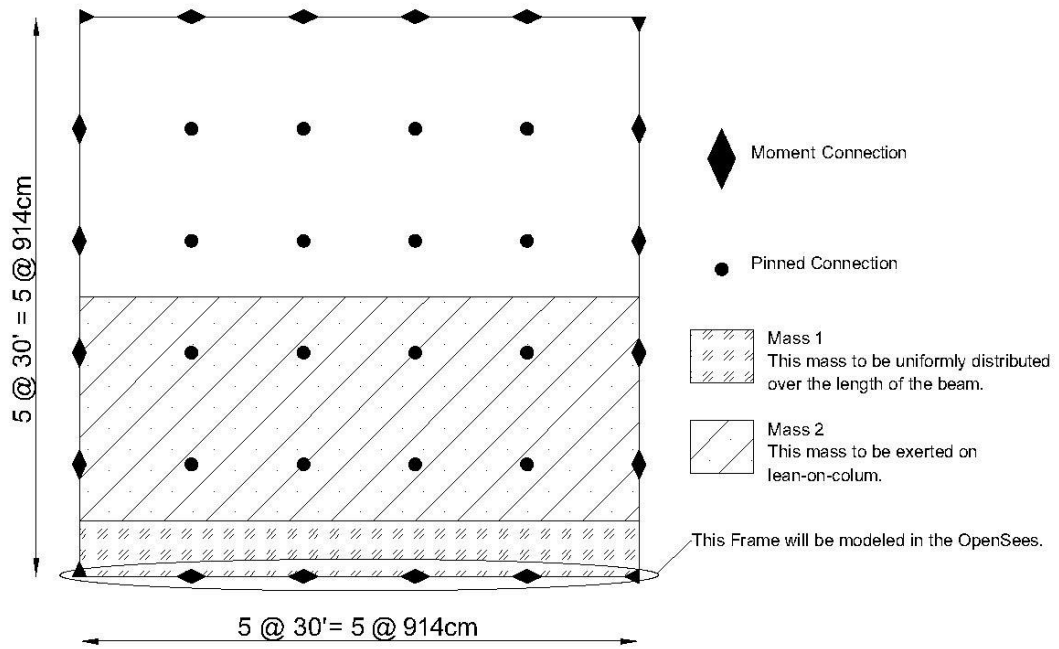


**Figure 2.5: Plan View and the Idealized Model of the 9-Story Building**

### 2.2.3 Model for Beam-Column Connections

In order to take into account the nonlinearity at beam-column connections, moment-rotation type connection model is employed in the thesis. For this purpose, one more node is introduced at the end of each beam that joins to the column. The coordinates of the new node are the same as the coordinate of the node that joins the beam to the column. Between these two nodes, a zero length element is introduced in OpenSees, where a moment-rotation type behavior is specified. For this purpose, the uniaxial hysteretic material model (*Hysteretic*) is considered to define the nonlinear and cyclic response of the connections. In this model, strength and stiffness degradation as well as pinching can be incorporated to the response of a connection (See Figure 2.6).

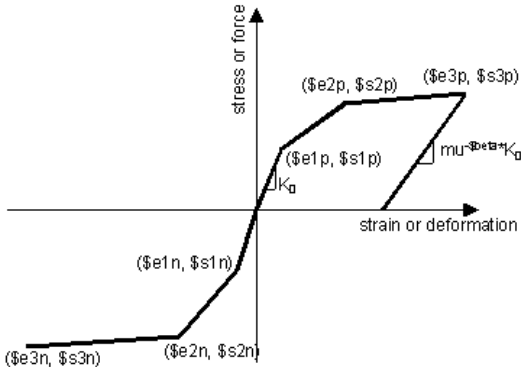


**Figure 2.6: Response of Hysteretic Material Model in OpenSees [42]**

A similar strategy for the simulation of nonlinear behavior of connections in steel framed structures was employed by Saritas and Koseoglu [5] through the use of a nonlinear force-based frame element, where it was shown in depth that the use of moment-rotation springs as outlined in here provides accurate response in predicting the nonlinear behavior of moment resisting steel framed structures with semi-rigid beam-column connections. Such a validation study is therefore not deemed necessary in this thesis and thus is not pursued.

For a special moment resisting frame (SMRF), the requirement for ductility as stated by Chen [49] outlines the performance of a connection to be capable of retaining 80% of its nominal strength at 0.04 rad rotation. A similar statement is also available in AISCI 341-16: the connections should preserve 80% of their ultimate moment carrying capacity at a drift angle of 0.04 [8]. The idealized acceptable response of a connection in moment resisting frame is shown in Figure 2.7 and this response is considered for the description of the nonlinear response of the connections in this thesis.

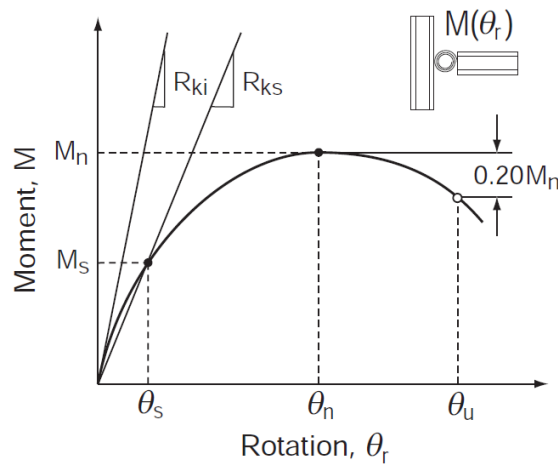


**Figure 2.7: Idealized Acceptable Response of a Connection in SMRF [48]**

The connections could be classified with respect to their stiffness as shown in the Table 2.11.  $M_n$  is the nominal capacity of a connection, and  $M_{p,beam}$  is the plastic moment capacity of the connecting beam. In this thesis, both the full and partial strength cases are considered in the parametric study, where the details are given in this section subsequently.

**Table 2.11: Connection Classification by Strength**

Connection	Strength
Full Strength (FS)	$M_n \geq M_{p,beam}$
Partial Strength (PS)	$M_n \leq M_{p,beam}$
No Strength	$M_n \leq 0.2 * M_{p,beam}$

The initial stiffness of connections is mostly expressed in terms of a multiple  $\lambda$  of the flexural stiffness  $(EI/L)_{\text{beam}}$  of the connecting beam, i.e. flexural rigidity  $EI$  of the beam divided to the length of the beam  $L$ . When  $\lambda$  is greater than 20, the connection stiffness is assumed to be close to the fully restraint case, thus rigid connection assumption is used for the sake of simplicity in practice. When  $\lambda$  is less than 2, the connection stiffness is assumed to be close to no rotation restraint case, i.e. simple connection assumption is employed. Any ratio that is between 2 and 20 is considered to fall into semi-rigid connection classification in terms of initial stiffness.

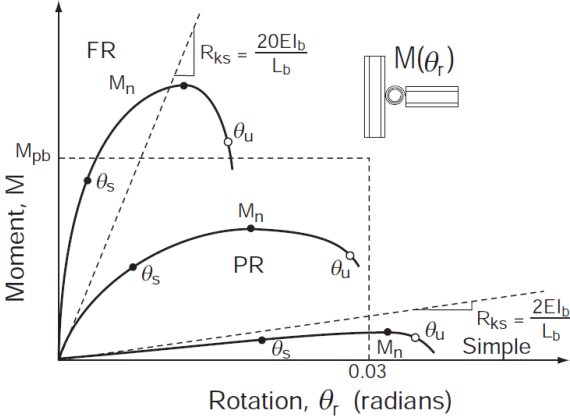


**Figure 2.8: Fully restrained (FR), PR, and simple connections [48]**

In Figure 2.8, these regions are presented for the distinction of the rigid, semi-rigid and simple connection response definitions based on initial stiffness of the connection. Evident from this plot, when the connection is actually assumed to be idealized as rigid, its response still contain nonlinearity and this might have a consequence on the overall response of a structural system. It is important to point out that a rigid connection in reality will have some flexibility, but more importantly, it will have a moment carrying and rotation capacity.

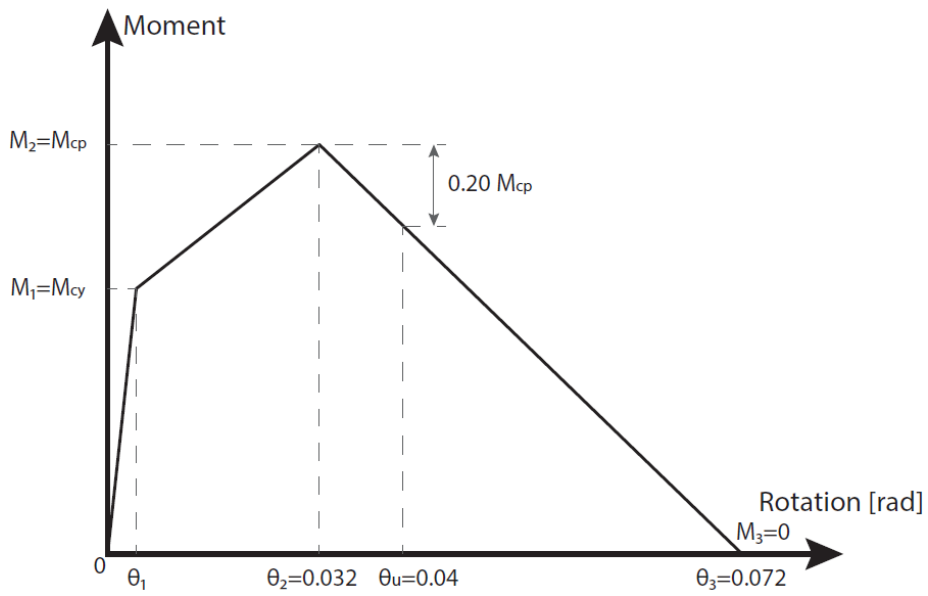
By using the above classifications and descriptions for the response of a connection, the following idealized multi-linear response is employed for a connection in this thesis. This response is provided as a moment-rotation model to the zero length elements joining the beam to the column in OpenSees. For the sake of meeting the ductility requirements as defined in Figure 2.7, strength loss in a connection is allowed

to take place as one of the cases of the parametric study. The pictorial view of the strength loss case is given in Figure 2.9a, where this response is assumed to satisfy the minimum lower bound requirement due to ductility. As an upper bound case for the parametric analysis, strength response for the connection is assumed to remain intact, i.e. no strength loss is assumed as shown in Figure 2.9b.

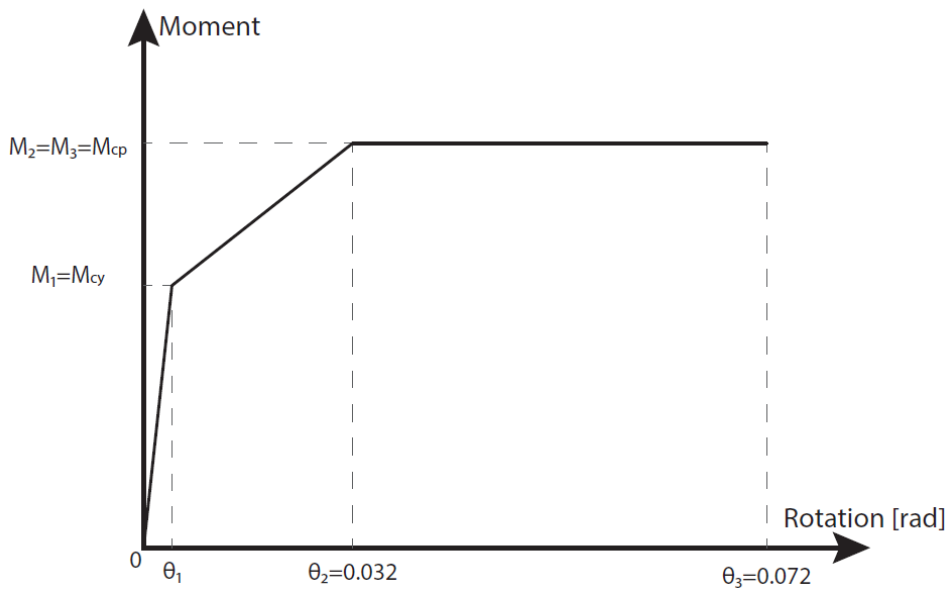
In this thesis, the ratio of the connection's yield moment capacity ( $M_1$ ) to their plastic moment capacity ( $M_2$ ) will be held constant at 0.67, which is the ratio of yield section modulus to plastic section modulus of the rectangular plate at the connection, thus reducing the number of parameters to vary in the analyses.

For the description of connection moment carrying capacity  $M_{cp}$ , three different parameters are used that are calculated from the joining beam's plastic moment capacity,  $M_{p,beam}$ . It is assumed that  $M_{cp}$  is set to 0.75, 1.1 or 1.45 multiple of  $M_{p,beam}$ . As a result, it is going to be possible to study both the full strength and partial strength cases mentioned in Table 2.11 for a connection.

In addition to the parameters defined above, two more behavior were also introduced to observe the importance of the hysteretic energy dissipation characteristic of a connection's nonlinear response. For this purpose, mild and severe pinching cases are considered. Mild pinching case is shown in Figure 2.10a. This case provides almost no loss of energy dissipation in repeated cycles of a connection's response. On the other hand, severe pinching case as shown in Figure 2.10b results into decrease in energy dissipation characteristic of a connection, where this can influence structural system performance that is only observable through a nonlinear time history analysis.

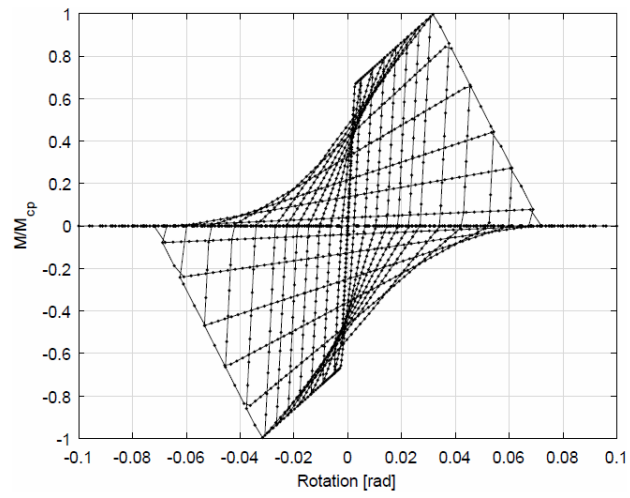


(a) With Strength Loss

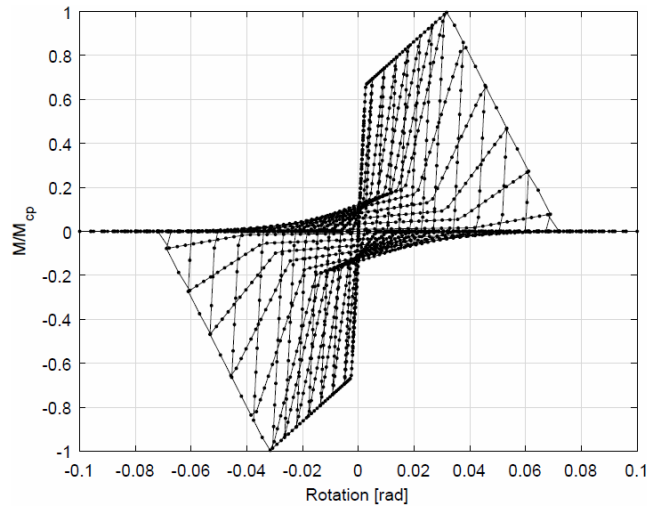


(a) Without Strength Loss

**Figure 2.9: Defined Spring Model in OpenSees**



(a) Mild Pinching with Strength Loss



(b) Severe Pinching with Strength Loss

**Figure 11: Presentation of Mild and Severe Pinching Cases for Connection Response under Strength Loss Case**



## CHAPTER 3

### OVERVIEW OF STRUCTURAL ANALYSIS TYPES

In this chapter, the structural analysis types used in this thesis are summarized. The mid-rise and high-rise buildings presented in Chapter 2 are parametrically studied in Chapter 4 by using push-over and nonlinear time history analyses. Before discussion of these analysis types, modal analysis is briefly mentioned, as well.

#### 3.1 Modal Analysis

Modal analysis provides the vibration characteristics, such as vibration periods (frequencies) and shapes, of structures mostly at the initial state, i.e. when the structure is linear elastic. In this thesis, modal analysis is also used for the determination of 1<sup>st</sup> mode shape of the structures, where this shape is considered as a load pattern for carrying out push-over analysis on the considered buildings in this thesis.

#### 3.2 Nonlinear Static (Push-Over) Analysis

Nonlinear static analysis, widely named as push-over analysis, provides practical analysis tool for the assessment of the nonlinear behavior of structures. Push-over analysis is carried out under the assumption that the response of a structure can be predicted closely with respect to the nonlinear (inelastic) time history analysis, where the latter provides a more realistic tool for the representation of a structure's behavior under seismic excitations.

Push-over analysis became quite popular due to its practicality, and due to the drawback of carrying out nonlinear time history analysis. In order to undertake nonlinear time history analysis, ground motion selection becomes an issue. Several time history analyses through the use of appropriately selected ground motions are needed in order to cause sufficient level of inelastic action on the considered structures. This necessitates the ground motions to be carefully selected in time history analysis [22] or by carrying out incremental dynamic analysis [47]. Despite this drawback, nonlinear time history analysis provides the real behavior of structures as a result of its capability to simulate stiffness, strength, inelasticity, as well as hysteretic response under cyclic excitations, as long as the structural model capabilities consider such actions. On the other hand, push-over analysis is actually only carried out in a monotonic fashion. A load pattern is needed to be selected, where this load pattern is successively increased in increments until the structure reaches a target displacement. Push-over analysis tries to mimic the lateral loading that might be caused by seismic excitation on a structure, but neglects the hysteretic actions due to load reversals.

Push-over analysis is expected to provide insight and information on a structure and its members with regards to

- Force demands
- Deformation demands
- Designation of critical regions.

In the literature, there is significant amount of effort in providing more reliable push-over analysis techniques. In this thesis, the use of 1<sup>st</sup> mode shape for the application of the lateral push-over load pattern on the structure is considered (Figure 3.1). This assumption assumes that the inertial actions on a structure impose the most dominant action in the 1<sup>st</sup> mode, and higher mode actions can be ignored, which is actually not true for high-rise structures. Other alternatives for load pattern application is the use of a uniform or triangular pattern as seen in Figure 3.1. Triangular pattern is mostly very close to the 1<sup>st</sup> mode pattern when the story masses and stiffness are similar. On the other hand, uniform load pattern imposes increased demands on a structure, which

may provide an upper bound estimate on push-over response [31]. Since the objective of this thesis was to use nonlinear time history analysis, the study of the effects of various load patterns in push-over analysis of considered buildings is not considered. Push-over analysis through the use of 1<sup>st</sup> mode pattern is only considered in this thesis in order to get an estimate of the nonlinear monotonic behavior of considered buildings, which may provide a practical comparison for the undertaken nonlinear time history analysis, as well.

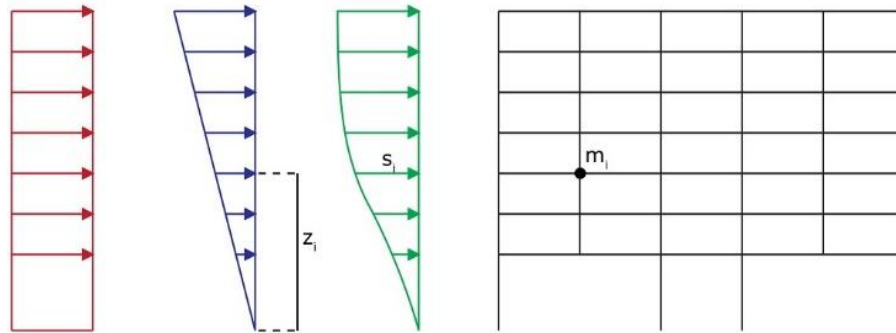


**Figure 12: Typical Load Patterns for Push-Over Analysis**

Although many advantages that this analysis offers, it has some drawbacks as well. Since the load is statically applied it can not thoroughly represent the dynamic case. Also, a single load pattern for a case with a rather weak top story, for which inertial forces would not be as much as the lower stories, would cause yielding in the top story columns but come short of creating yielding at the lower stories. In general, the most crucial problem could be that this type of analysis could capture the first yielding mechanism and can not proceed to the successive mechanism in case of which the structure's dynamic response change due to redistribution.

### 3.3 Nonlinear Time History Analysis

In a nonlinear time history analysis, several ground motion records are needed to be used in order to cause desired target of demands on a structure. Although this requires more time and effort than push-over analysis, nonlinear time history analysis is the most accurate method for the determination of the overall inelastic behavior of a structural system. Ground motion selection in this regards becomes a critical issue. In this thesis, two set of 20 ground motions presented in the report SAC/BD-97/04 are imposed on the structures [34]. For these 40 ground motions, the target spectra was modified to be representative for stiff soil, and it is stated that the shear wave velocity is between 183 m/sec and 366 m/sec. 1<sup>st</sup> group of data set has 10% of probability of exceedance, and the 2<sup>nd</sup> is scaled in order to match a 2% of probability in 50 years. Under the 1<sup>st</sup> group the structures is expected not to collapse but for the 2<sup>nd</sup> group the mere concern is the safe eviction of the occupants. 4.3% of damping is assigned in the analysis. The table for the ground motions and their response spectra is given on the following tables and figures.

In carrying out time history analysis, it is also necessary to use elastic damping in order to take into account the effects of energy dissipation due to various actions that take place in a structure before the load carrying members go into inelastic action. The level of elastic damping is mostly taken closer to 5% in reinforced concrete structures and 2% in steel structures with welded connections. Elastic damping not only provides the elastic energy dissipation in load carrying members, but it can also reflect the energy dissipation in all non-structural components, as well. Furthermore, the fact that a steel structure incorporates partially restraint connections with bolts also contributes additional elastic energy dissipation at connection regions. In the study of Lee and Foutch [25], the level of damping was taken as 4.3% for the low-rise SAC moment resisting frames, while this value was reduced for mid-rise to 3.6% and 2.3% for high-rise buildings, which is actually not a typical approach to undertake. In a previous study, Karakas studied the low-rise SAC buildings with 4.3% elastic damping. In this thesis, the level of damping is not changed as story height changes, and a fixed value

of 4.3% Rayleigh damping is considered for the mid-rise and high-rise buildings, as well.

**Table 3.1: Los Angeles (LA) ground motions for the 10% in 50 years hazard**

<b>EQ Code</b>	<b>Record</b>	<b>Earthquake Magnitude (M<sub>w</sub>)</b>	<b>Distance (km)</b>	<b>Scale Factor</b>	<b>Number of Points</b>	<b>Time Step (s)</b>	<b>Duration (s)</b>	<b>PGA (g)</b>
LA01	Imperial Valley, 1940, El Centro	6.9	10	2.01	2674	0.02	53.46	0.46
LA02	Imperial Valley, 1940, El Centro	6.9	10	2.01	2674	0.02	53.46	0.68
LA03	Imperial Valley, 1979, Array #05	6.5	4.1	1.01	3939	0.01	39.38	0.39
LA04	Imperial Valley, 1979, Array #05	6.5	4.1	1.01	3939	0.01	39.38	0.49
LA05	Imperial Valley, 1979, Array #06	6.5	1.2	0.84	3909	0.01	39.08	0.3
LA06	Imperial Valley, 1979, Array #06	6.5	1.2	0.84	3909	0.01	39.08	0.23
LA07	Landers, 1992, Barstow	7.3	36	3.2	4000	0.02	79.98	0.42
LA08	Landers, 1992, Barstow	7.3	36	3.2	4000	0.02	79.98	0.43
LA09	Landers, 1992, Yermo	7.3	25	2.17	4000	0.02	79.98	0.52
LA10	Landers, 1992, Yermo	7.3	25	2.17	4000	0.02	79.98	0.36
LA11	Loma Prieta, 1989, Gilroy	7.0	12	1.79	2000	0.02	39.98	0.67
LA12	Loma Prieta, 1989, Gilroy	7.0	12	1.79	2000	0.02	39.98	0.97
LA13	Northridge, 1994, Newhall	6.7	6.7	1.03	3000	0.02	59.98	0.68
LA14	Northridge, 1994, Newhall	6.7	6.7	1.03	3000	0.02	59.98	0.66
LA15	Northridge, 1994, Rinaldi RS	6.7	7.5	0.79	2990	0.005	14.945	0.53
LA16	Northridge, 1994, Rinaldi RS	6.7	7.5	0.79	2990	0.005	14.945	0.58
LA17	Northridge, 1994, Sylmar	6.7	6.4	0.99	3000	0.02	59.98	0.57
LA18	Northridge, 1994, Sylmar	6.7	6.4	0.99	3000	0.02	59.98	0.82
LA19	North Palm Springs, 1986	6.0	6.7	2.97	3000	0.02	59.98	1.02
LA20	North Palm Springs, 1986	6.0	6.7	2.97	3000	0.02	59.98	0.99

**Table 3.2: Los Angeles (LA) ground motions for the 2% in 50 years hazard level**

<b>EQ Code</b>	<b>Record</b>	<b>Earthquake Magnitude (M<sub>w</sub>)</b>	<b>Distance (km)</b>	<b>Scale Factor</b>	<b>Number of Points</b>	<b>Time Step (s)</b>	<b>Duration (s)</b>	<b>PGA (g)</b>
LA21	1995 Kobe	6.9	3.4	1.15	3000	0.02	59.98	1.28
LA22	1995 Kobe	6.9	3.4	1.15	3000	0.02	59.98	0.92
LA23	1989 Loma Prieta	7.0	3.5	0.82	2500	0.01	24.99	0.42
LA24	1989 Loma Prieta	7.0	3.5	0.82	2500	0.01	24.99	0.47
LA25	1994 Northridge	6.7	7.5	1.29	2990	0.005	14.945	0.87
LA26	1994 Northridge	6.7	7.5	1.29	2990	0.005	14.945	0.94
LA27	1994 Northridge	6.7	6.4	1.61	3000	0.02	59.98	0.93
LA28	1994 Northridge	6.7	6.4	1.61	3000	0.02	59.98	1.33
LA29	1974 Tabas	7.4	1.2	1.08	2500	0.02	49.98	0.81
LA30	1974 Tabas	7.4	1.2	1.08	2500	0.02	49.98	0.99
LA31	Elysian Park (simulated)	7.1	17.5	1.43	3000	0.01	29.99	1.3
LA32	Elysian Park (simulated)	7.1	17.5	1.43	3000	0.01	29.99	1.19
LA33	Elysian Park (simulated)	7.1	10.7	0.97	3000	0.01	29.99	0.78
LA34	Elysian Park (simulated)	7.1	10.7	0.97	3000	0.01	29.99	0.68
LA35	Elysian Park (simulated)	7.1	11.2	1.1	3000	0.01	29.99	0.99
LA36	Elysian Park (simulated)	7.1	11.2	1.1	3000	0.01	29.99	1.1
LA37	Palos Verdes (simulated)	7.1	1.5	0.9	3000	0.02	59.98	0.71
LA38	Palos Verdes (simulated)	7.1	1.5	0.9	3000	0.02	59.98	0.78
LA39	Palos Verdes (simulated)	7.1	1.5	0.88	3000	0.02	59.98	0.5
LA40	Palos Verdes (simulated)	7.1	1.5	0.88	3000	0.02	59.98	0.63

While this value of damping is higher than the usual value taken in practice, this will allow us to relate the results of our study for mid-rise and high-rise with the study of Karakas for low-rise. The parametric study is undertaken for both the rigid connection and partially restraint connection cases, and the results will be comparable as long as a constant damping is considered for the representation of elastically dissipated seismic energy.

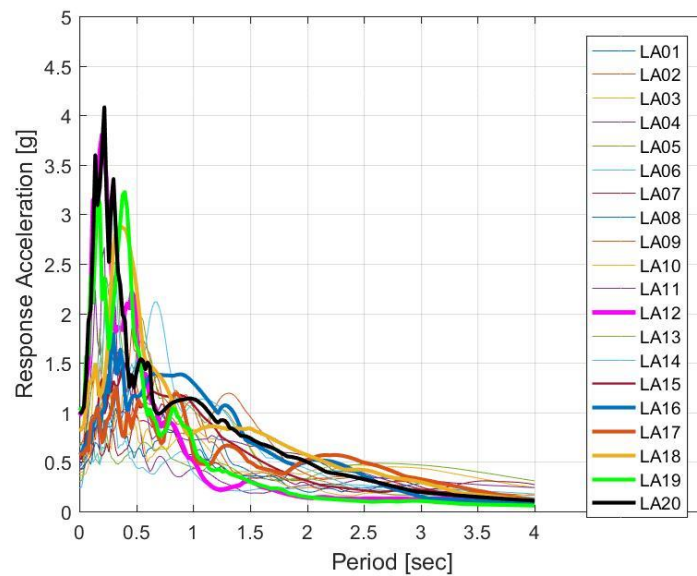


**Figure 13: Response Spectra for the 1st set of Ground Motion Data**

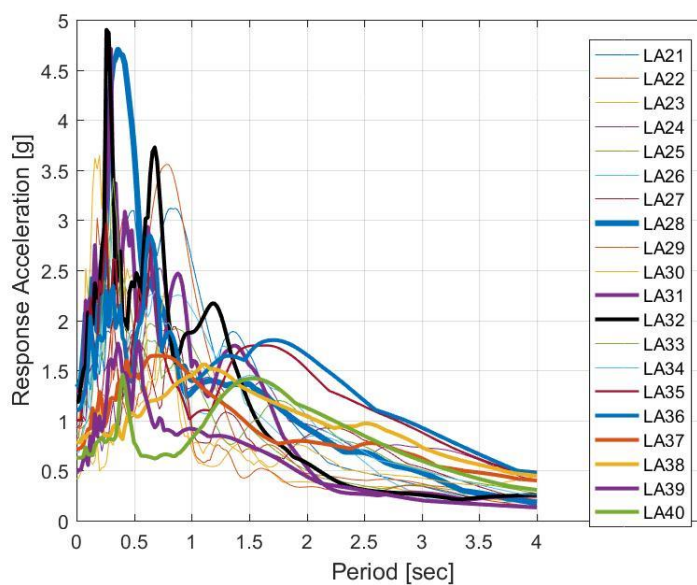


**Figure 14: Response Spectra for the 2nd set of Ground Motion Data**

In the next chapter, the displacements in terms of inter-story drift ratios caused in the buildings due to the use of presented ground motions in Table 3.1 and Table 3.2 will be compared with the performance levels defined by FEMA 356, and these are presented below and detailed in Table 3.3:

- **Immediate Occupancy**, where the structure continues to serve without any damage or very little damage.
- **Damage Control Range**, where the phase in between Immediate Occupancy level and Life Safety is defined. The structure is expected to operate as fast as possible after the repair.
- **Life Safety**, where there could be some local damages but the overall structure standing.
- **Limited Safety Range**, where the phase in between Life Safety and the Collapse Prevention is defined.
- **Collapse Prevention**, where the building remains standing but the structural elements are damaged in excessive range.
- **Not Considered**, where the structure is heavily damaged that no repair is addressed.

**Table 3.3: Drift Ratios by Structural Performance Level for Steel Moment Frames in FEMA 356**

Structural Performance Level	Drift Ratio (%)	
	Transient	Permanent
Immediate Occupancy Level (S-1)	0.7	Negligible
Life Safety Level (S-3)	2.5	1.0
Collapse Prevention Level (S-5)	5.0	5.0

## CHAPTER 4

### RESULTS OF PARAMETRIC STUDY

In this chapter results of the push-over and nonlinear time history analyses of the mid-rise and high-rise buildings will be presented. The results will be demonstrated in terms of base shear versus roof drift for the push-over analysis, and inter-story drift ratio profiles for the nonlinear time history analysis. The effects of the upper bound and the lower bound design of the buildings will be discussed, as well as the attributed properties, which are the presence of the strength loss and severe pinching in the connection, the stiffness and the strength of the connection, on the behavior of the structure will be sought for the considered buildings. Lastly, there will be a comparison with the influence of above aspects observed in low-rise buildings studied by Karakas[50].

The selected parameters that will represent the nonlinear behavior of each connection result into 12 different cases for each analyzed building, besides the rigid connection case. The initial stiffness ratio  $\lambda$  of the connections is 15 in all 12 cases for a building, where  $\lambda$  is obtained by dividing the initial stiffness of the connection to the flexural stiffness  $EI/L$  of the beam. This ratio is actually close to the rigid connection limit of 20. The connection's moment capacity  $M_{cp}$  is calculated as a factor  $\beta$  of the plastic moment capacity of the beam under zero axial load, denoted as  $M_{p,beam}$ . The factor  $\beta$  is varied as 0.75, 1.1 or 1.45. Selection of 0.75 results into partial strength connection, and the selection of 1.45 ensures full strength connection. Since there is strain hardening of 0.03 considered for the steel material in the members, the moment capacity of the beam under zero axial load will increase above  $M_{p,beam}$ , and the selection of  $\beta = 1.1$  yields approximately the same peak moment capacity for the connection and the beam that has hardened, though not happening at the same time.

The details of the monotonic backbone curve of the moment-rotation behavior of the connections are presented in Chapter 2. The connection peak strength  $M_{cp}$  once reached is assumed to follow either zero hardening (no strength loss case) or drop to 80% of  $M_{cp}$  at a value 0.04 connection rotation by satisfying ductility requirements, where the latter case is named as strength loss case. A final parameter is considered for the nonlinear time history analysis, that is the pinching characteristic of the hysteretic response of the connection. For the variation in pinching, mild and severe cases are considered, where details of the response were provided in Chapter 2.

For the mid-rise buildings, above cases are considered for both the lower bound (LB) and upper bound (UB) designed versions of the buildings. The resulting cases for the mid-rise building are numbered as given in Table 4.1, in total resulting to 26 cases. For the high-rise building, there is only one version of design due to the height of the building, and the resulting 13 model cases for high-rise building are provided in Table 4.2.

**Table 4.1: List of Models for the 9-Story Building**

W14 Lower Bound					W36 Upper Bound				
Model #	$\lambda$	$\beta$	Strength Loss	Pinching	Model #	$\lambda$	$\beta$	Strength Loss	Pinching
1	15	0.75	Yes	Mild	13	15	0.75	Yes	Mild
2	15	0.75	Yes	Severe	14	15	0.75	Yes	Severe
3	15	0.75	No	Mild	15	15	0.75	No	Mild
4	15	0.75	No	Severe	16	15	0.75	No	Severe
5	15	1.1	Yes	Mild	17	15	1.1	Yes	Mild
6	15	1.1	Yes	Severe	18	15	1.1	Yes	Severe
7	15	1.1	No	Mild	19	15	1.1	No	Mild
8	15	1.1	No	Severe	20	15	1.1	No	Severe
9	15	1.45	Yes	Mild	21	15	1.45	Yes	Mild
10	15	1.45	Yes	Severe	22	15	1.45	Yes	Severe
11	15	1.45	No	Mild	23	15	1.45	No	Mild
12	15	1.45	No	Severe	24	15	1.45	No	Severe
25	RIGID CASE for W14				26	RIGID CASE for W36			

**Table 4.2: List of Models for the 20-Story Building**

W14				
Model	$\lambda$	$\beta$	Strength Loss	Pinching
1	15	0.75	Yes	Mild
2	15	0.75	Yes	Severe
3	15	0.75	No	Mild
4	15	0.75	No	Severe
5	15	1.1	Yes	Mild
6	15	1.1	Yes	Severe
7	15	1.1	No	Mild
8	15	1.1	No	Severe
9	15	1.45	Yes	Mild
10	15	1.45	Yes	Severe
11	15	1.45	No	Mild
12	15	1.45	No	Severe
13	RIGID CASE for W14			

#### 4.1 Fundamental Periods of the Considered Buildings

The fundamental natural periods of the model cases presented in Tables 4.1 and 4.2 are provided in Table 4.3 for the mid-rise and high-rise buildings, respectively. The periods are obtained by carrying out modal analysis considering the initial stiffness of the structure. The difference between the semi-rigid to rigid cases are given, as well.

**Table 4.3: The First Periods of the 9-Story Building**

9-Story (Mid-rise) Building - W14 Lower bound design				
Model #	T (sec)	Model #	T (sec)	Difference
1 to 12 (Semi-rigid)	2.71	25 (Rigid)	2.42	12.1%
9-Story (Mid-rise) Building - W36 Upper bound design				
Model #	T (sec)	Model #	T (sec)	Difference
13 to 24 (Semi-rigid)	2.62	26 (Rigid)	2.15	21.4%
20-Story (High-rise) Building - W14				
Model #	T (sec)	Model #	T (sec)	Difference
1 to 12 (Semi-rigid)	3.73	25 (Rigid)	3.42	9.0%

In a previous study for low-rise buildings by Karakas [50], the difference between semi-rigid cases of the buildings for both LB and UB designed cases was approximately 8.5%. For the considered mid-rise and high-rise buildings, connection flexibility resulted into approximately in the same level of increase except than the upper bound designed mid-rise structure. In the upper bound designed 9-story building, the change in fundamental period in semi-rigid case reached to 21% with respect to the rigid case. This drastic change is actually due to the fact that the beam sizes are not enlarged as much as the columns, therefore the flexibility at the connection region resulted into increased change in the 1<sup>st</sup> period. It is worth to point out that the increase in the structural periods of the mid-rise and high-rise buildings may possibly result into attracting less seismic forces when time history analysis is carried out, where this can be realized from the response spectra curves in Chapter 3.

#### **4.2 Push-Over Analysis Results for the 9-Story Buildings**

In this part, the curves generated from the push-over analysis of the 9-story buildings will be presented for the model cases given in Table 4.1. It is worth to emphasize that it is not possible to study the influence of pinching behavior in a monotonic analysis. Push-over analysis of the buildings were undertaken by applying 1<sup>st</sup> mode shape obtained from modal analysis as a lateral load pattern on the buildings. Details about the push-over analysis was provided in Chapter 2. The roof drift of the structures are all increased upto 6% provided that the solution converges.

First, the rigid case results for the upper bound (UB) and lower bound (LB) designed versions of 9-story building are presented in terms of base shear versus roof drift ratio in Figure 4.1. Base shear values are divided to the seismic weight of the structure in order to get a non-dimensional result in the y-axis. It is evident from Figure 4.1 that UB design case has higher stiffness and strength than the LB design case. The influence of nonlinear geometric effects is evident from the softening in stiffness after peak, however it is not at a pronounced level for these buildings.

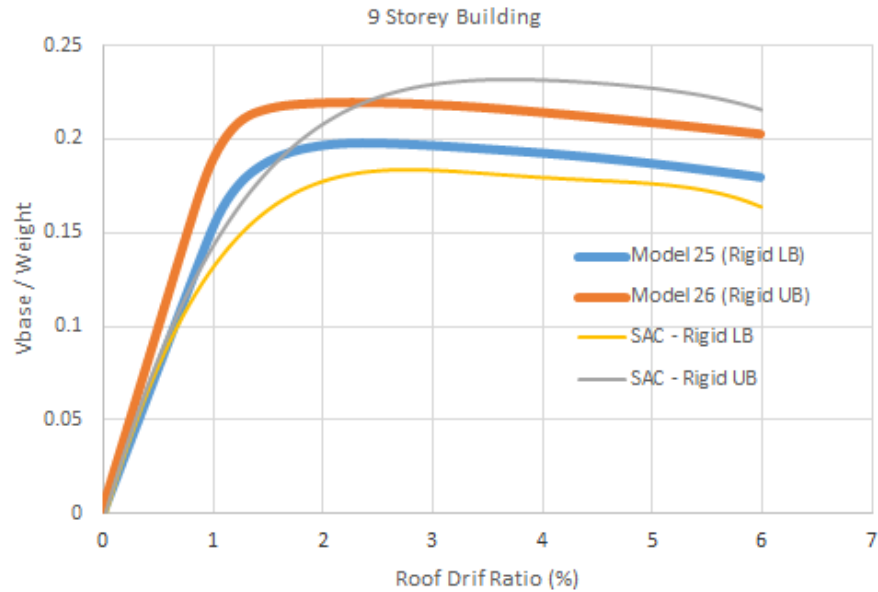


**Figure 4.1: Push-Over Curves for the Rigid Cases (LB and UB)**

After presentation of the basic differences between lower bound and upper bound designed buildings, now the influence of connection nonlinearity will be investigated. For this purpose, the responses of lower bound and upper bound design structures will be presented separately.

In Figure 4.2, push-over curves for LB designed 9-story building are plotted for no strength loss cases for the connections in Table 4.1. For this presentation, plastic moment capacity for the connection is considered to change 0.75, 1.10 and 1.45 times the  $M_{p,beam}$ , where these models were numbered as Models 3,7 and 11, respectively, in Table 4.1. In Figure 4.2, result of the LB designed rigid case is also provided. The results of the semi-rigid cases' initial stiffness is slightly less than the rigid case. It is evident that connection strength plays a significant role in the nonlinear behavior of the structure. Due to yielding at the connections, push-over curves show drastic change from the elastic to plastic branch. For Model 3, with the moment strength that is 70% of the connecting beams' plastic capacity, it is observed that the ultimate load carrying capacity has dropped down to 50% of the rigid frame.

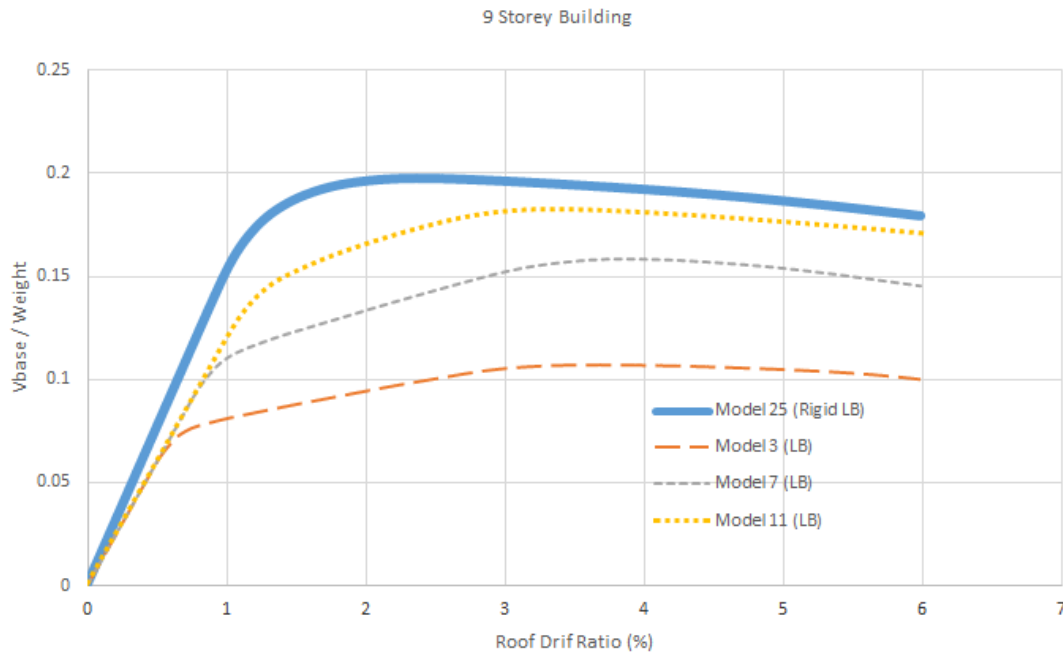


**Figure 4.2: Push-Over Curves for the LB 9-Story Buildings without Strength Loss**

Next, the influence of connection strength loss on the nonlinear behavior of the LB designed mid-rise building will be presented. Push-over analysis results obtained from Models 2, 6 and 10 are plotted in Figure 4.3, where these models all consider strength loss with varying connection moment capacities of 0.70, 1.1 or 1.45 times of plastic moment capacity of connection beam, respectively. For the sake of comparison, rigid case result, as well as Model 3 result, i.e. partial connection strength and no connection loss case, are also provided.

The trend in the peak load carried by the semi-rigid cases in Models 2, 6 and 10 resemble the results attained in Figure 4.2, except than the sudden loss of strength caused in the load carrying capacity of the structures due to the loss of strength after 3% roof drift ratio. Influence of strength loss is more evident from the comparison of the responses of Models 2 and 3. As a result of the nonlinear geometric effects, the overall stability of the structures are significantly affected by the loss of strength in the connection. It is important to point out that the level of strength loss in the structures was provided such that ductility requirements at the connection were met.

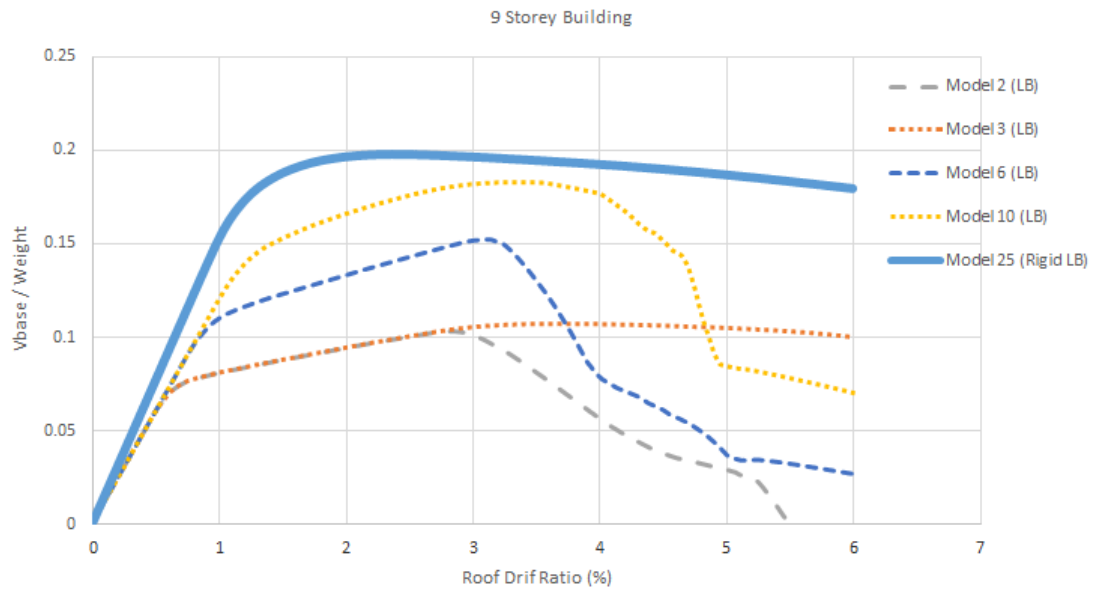


**Figure 4.3: Push-Over Curves for LB 9-Storey Buildings with Strength Loss**

Same fashion is observed for the upper bound design (UB) frames, as well, apart from the fact that they all have higher load capacity for any roof drift ratio. The results of push-over analysis of UB designed 9-story building can be seen in Appendix.

#### 4.3 Push-Over Analysis Results for the 20-Story Building

Results of the push-over analysis of 20-story building are given again in terms of base shear versus roof drift ratio by applying the 1<sup>st</sup> mode eigen-vector as a load pattern on the structure. The high-rise building has only one design version, therefore the result of the rigid case will be directly presented with the semi-rigid cases.

Push-over curves of the semi-rigid cases with no strength loss are presented in Figure 4.4 and compared with the rigid case. It is evident that the initial stiffness of the rigid and semi-rigid cases are very close to each. Furthermore, due to height and influence of nonlinear geometric effects, the push-over curves demonstrate significant loss of

stability resulting into negative stiffness after peak load. Similar to the mid-rise building, partial strength response of the connection resulted into close to 50% loss of load carrying capacity for the structure when compared with the rigid case.

It is worth to look at the results for the high-rise building with caution due to the fact that 1<sup>st</sup> mode shape is used for applying the lateral load on the structure. For high-rise buildings, higher mode effects could become pronounced and actually these effects can be studied in a more accurate way through time history analysis.

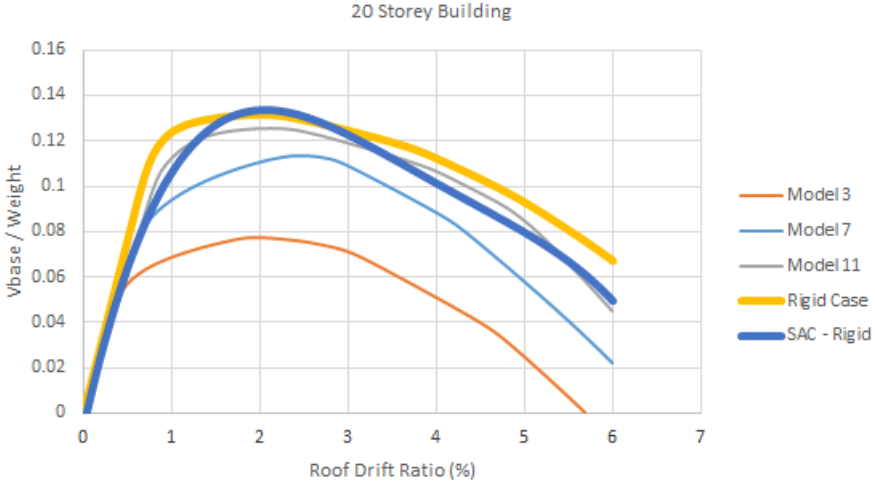


**Figure 4.4: Push-Over Curves for 20-Story Buildings without Strength Loss**

Next, the influence of connection strength loss on the nonlinear behavior of the 20-story building will be presented. Push-over analysis results obtained from Models 2, 6 and 10 are plotted in Figure 4.5, and these models consider strength loss with varying connection moment capacities of 0.70, 1.1 or 1.45 times of plastic moment capacity of connection beam, respectively. For the sake of comparison, rigid case result, as well as Model 3 result, i.e. partial connection strength and no connection loss case, are also provided. Evident from the figure that strength loss in the connections can only be tolerated when connection moment capacity is much higher compared to the beam capacity. For equivalent and partial strength connections, strength loss results into sudden drop of load carrying capacity of the structure approximately at 2% roof drift ratio.

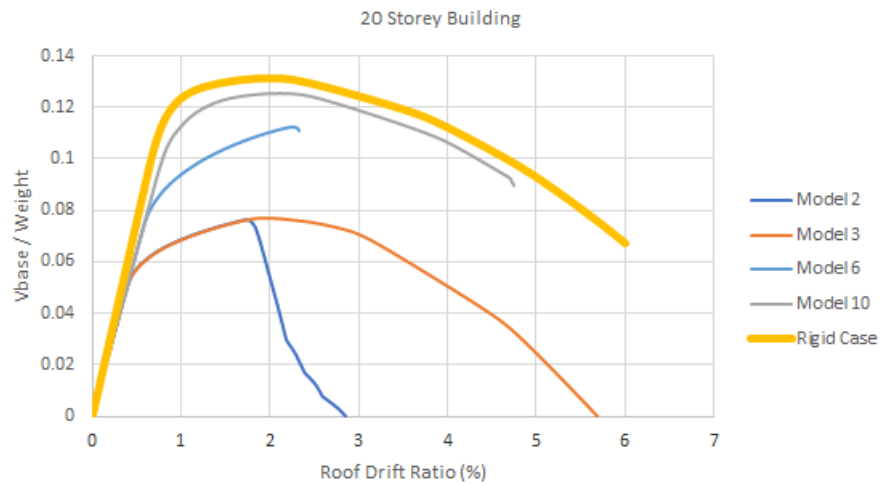


**Figure 4.5: Push-Over Curves for 20-Story Buildings with Strength Loss**

In Figure 4.5, rigid case and Model 3 results are also presented for the sake of providing comparison. Model 2, which is same with Model 3 apart from having strength loss, experience a sudden drop of load capacity close to 2% roof drift due to the loss of strength at connection regions. Model 6 also experiences sudden strength drop close to 2% roof drift ratio. On the other hand, it is evident that if connection strength is much higher than beam strength as in Model 10, this delays the sudden drop in capacity due to connection strength loss to 5 % roof drift ratio. From the push-over analysis, one can deduce that the use of connections with strength loss should be approached with caution, and in that case the use of full strength connections is advised in order to delay possible failure at lower drifts.

### 4.3 Non-Linear Time History Analysis Results

In carrying out time history analysis, 2 sets of 20 ground motions that were presented in Chapter 3 are used, where these sets represent 10% and 2% probability of exceedance in 50 years. In total, there are 1040 and 520 nonlinear time history analyses for the mid-rise and high-rise buildings, respectively.

As mentioned earlier, due to inclusion of higher mode effects, push-over analysis underestimates the ultimate load carrying capacity of the structures. This could be seen on Figure 4.6 on which nonlinear time history analysis results are plotted along with the push-over curve for the rigid lower bound model of 9-story building and rigid model of the 20-story building.

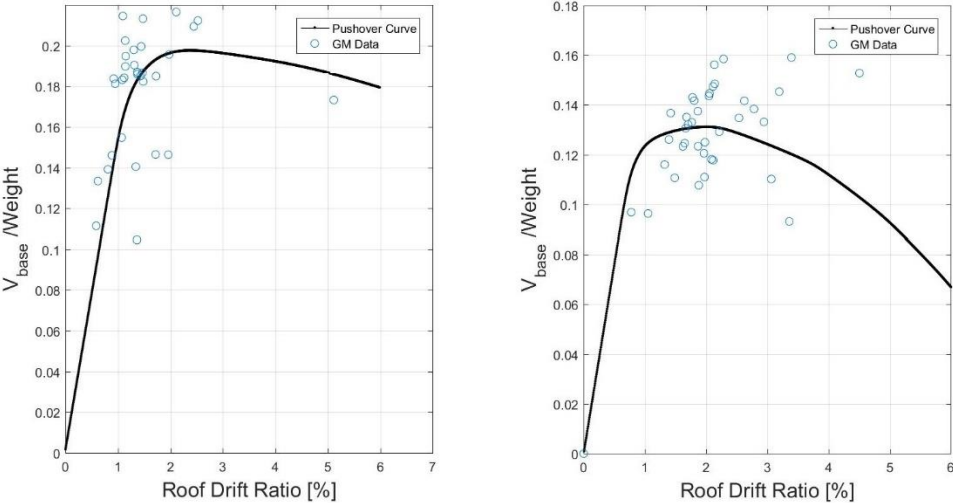


**Figure 4.6: Nonlinear Time History and Push-over Analyses Results for Rigid Buildings of 9-Story (Left) and 20-Story (Right)**

In above figure, it can be seen that push-over analysis underestimates the ultimate load bearing capacity of the 9-story building by a factor of 10% approximately. This ratio, gets even larger for the 20-story building, and is around 25%. This discrepancy is due to higher mode effects, and the reduction of mass participation at the 1st mode, where this mode was imposed on the push-over analyses. For the 9-story building, the mass participation is close to 85% from 1st mode, whereas for the 20-story building this ratio is close to 80%. It is evident that higher mode shapes should have been taken into account in carrying out the push-over analyses of these buildings. The higher mode effect could also be observed from the figures showing the interstory drift ratios at the end of this chapter. The absolute maximum values of the base shear and absolute maximum values of the roof drift ratio, plotted in Figure 4.6, happen at different instances during a particular ground motion record. In most ground motion records,

absolute maximum base shear happens shortly after the occurrence of peak ground acceleration (PGA). On the other hand, the absolute maximum drift takes place much after the occurrence of PGA, as ground excitation continues. In order to clarify this point, the response of the 9-story building for Model 17 under LA40 from time history analysis is presented in Figure 4.7 along with its push-over curve. A one to one direct comparison of time history analysis is usually not possible, but it is evident that the strength loss in the structure is clearly visible in the time history plot in Figure 4.7.

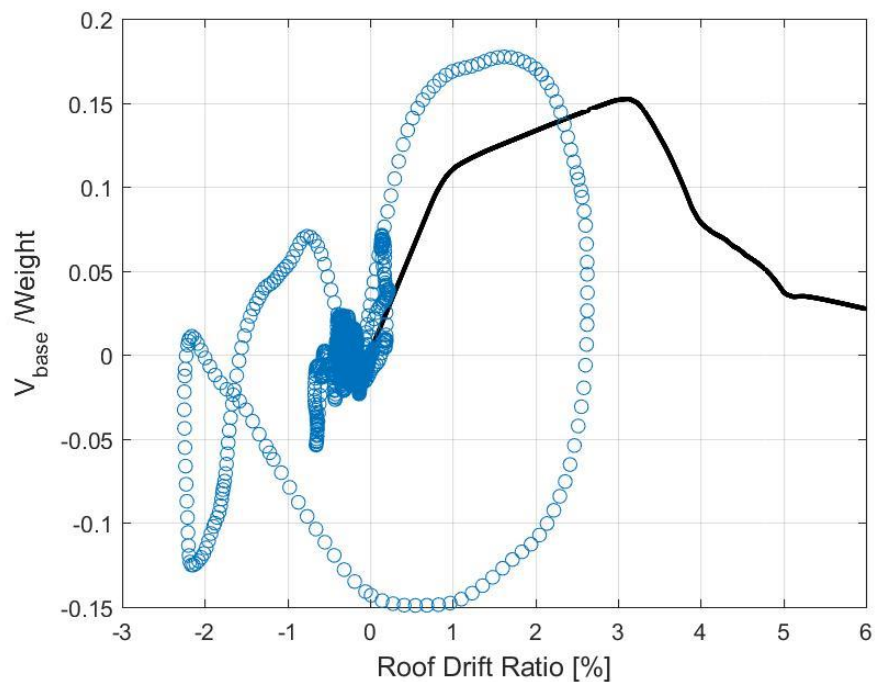


**Figure 4.7: Push-over Analysis (PA) and Nonlinear Time History Analysis (NTHA) Results of Model 17 for 9-Story Building subjected to LA40 (continuous curve: PA, dotted curve: NTHA)**

Nonlinear time history analyses are mostly used in order to point out the most relevant parameter in the performance assessment of structural systems, that is the level of inter-story drift ratio (IDR). It was mentioned in Chapter 3 that the performance levels set by FEMA 256 document outline 2.5% and 5.0% inter-story drift limits for life safety and collapse prevention levels, respectively. In carrying out time history analysis, the influence of pinching in connection behavior can be assessed, and its contribution can be quantified from the changes in IDR. Furthermore, an accurate

representation of higher mode effects on the 20-story building will be obtained by carrying out time history analysis.

The results of the nonlinear time history analysis of the 26 models for the 9-story buildings and 13 models for the 20-story building are tabulated for the sake of simplicity in this chapter, in Tables 4.1 and Table 4.2 in terms of absolute maximum IDR. Story wise distribution of IDR profiles are also provided at the end of the chapter.

First, the maximum values for the median IDR values will be tabulated for the 9-story buildings. In Table 4.4, the median of the maximum absolute values of IDR obtained from the 40 ground motion simulations through the height of each model case are presented. It can be seen that for each model case, life safety limit is not exceeded even when there is loss of connection strength.

Lower bound design structures in overall resulted in increased median IDR values compared to the upper bound design, but the response appears to be especially insignificant for Models 1-8 and Models 13-20, i.e. for partial and equal strength connections. On the other hand, for full strength connection case, the fact that upper bound design is chosen has an importance when compared with the lower bound design. The most significant effect is observed for the strong connection cases with severe pinching in Models 10 and 12. It can be seen that lower bound designed structure experiences 20% more displacement compared to the upper bound design when pinching is severe in both. It can be concluded that upper bound design in overall provides a more reliable nonlinear response.

Results are also compared with the median IDR values obtained for the rigid cases, and approximately 30% increase in displacement demands are observed. Evident from Table 4.4 is the slight influence of pinching on increased displacement demands on the structure. The gray results are the severe pinching cases, and one row about each represent everything the same except than the fact that pinching is mild.

**Table 4.4: Maximum Median of IDR Values of the 9-Story Building**

Median of IDR Values of the 9-Story Building						
Lower Bound Design			Upper Bound Design			LB/UB
Model	$\Delta$ (IDR)	$\Delta_i /$ $\Delta_{rigid}$	Models	$\Delta$ (IDR)	$\Delta_i /$ $\Delta_{rigid}$	$\Delta_{LB} /$ $\Delta_{UB}$
1	2.19	1.28	13	2.19	1.32	1.00
2	2.34	1.36	14	2.32	1.40	1.01
3	2.21	1.29	15	2.19	1.32	1.01
4	2.38	1.39	16	2.32	1.40	1.02
5	2.17	1.26	17	2.07	1.25	1.05
6	2.25	1.31	18	2.15	1.29	1.05
7	2.17	1.26	19	2.07	1.25	1.05
8	2.25	1.31	20	2.15	1.29	1.05
9	2.20	1.28	21	2.04	1.23	1.08
10	2.36	1.38	22	1.96	1.18	1.20
11	2.20	1.28	23	2.04	1.23	1.08
12	2.36	1.38	24	1.96	1.18	1.20
25 (Rigid)	1.71	1.00	26 (Rigid)	1.66	1.00	1.03

Median values are popularly used since they provide a more highly likely occurrence of a structure's demand for a given set of ground motions. Despite this, in order to impose stricter limits, the performance level of a building should actually be satisfied for most of the ground motions considered for the time history analysis. It is true that the second set of ground motions probability of exceedance is low, yet in the event of the maximum earthquake, these displacement demands will become more critical in assessing the performance of a building. For this purpose, 84<sup>th</sup> percentile of the IDR values obtained from each model case will be presented below.

Table 4.5 shows the maximum of the 84<sup>th</sup> percentile values of the IDR for each model case for both lowerbound and upper bound designed 9-story buildings. All of the IDR values are above the life safety level of 2.5% for all cases, but at the same time, are below the collapse prevention level of 5% as stated in FEMA 356. Severe pinching

results in 20% higher IDR for the upper bound design cases. For the upper bound design cases, except the models where the connection’s moment capacity is as much as the beam’s capacity (Models 9-12), the increase in the IDR with respect to the rigid case is higher than the lower bound design.

**Table 4.5: Maximum of the 84<sup>th</sup> Percentile of IDR Values of the 9-Story Building**

84th Percentile of IDR Values of the 9 Story Building						
Lower Bound Design			Upper Bound Design			LB/UB
Model	$\Delta$ (IDR)	$\Delta_i / \Delta_{rigid}$	Models	$\Delta$ (IDR)	$\Delta_i / \Delta_{rigid}$	$\Delta_{LB} / \Delta_{UB}$
1	3.06	1.07	13	3.32	1.21	0.92
2	3.04	1.07	14	3.95	1.44	0.77
3	3.03	1.06	15	3.32	1.21	0.91
4	3.05	1.07	16	3.96	1.45	0.77
5	3.17	1.11	17	3.42	1.25	0.93
6	3.33	1.17	18	3.67	1.34	0.91
7	3.17	1.11	19	3.42	1.25	0.93
8	3.33	1.17	20	3.67	1.34	0.91
9	3.28	1.15	21	3.13	1.15	1.05
10	3.52	1.23	22	2.97	1.09	1.18
11	3.28	1.15	23	3.13	1.15	1.05
12	3.52	1.23	24	2.97	1.09	1.18
25 (Rigid)	2.85	1.00	26 (Rigid)	2.73	1.00	1.04

The figures for the IDR profiles of the models with and without strength loss are also provided below.

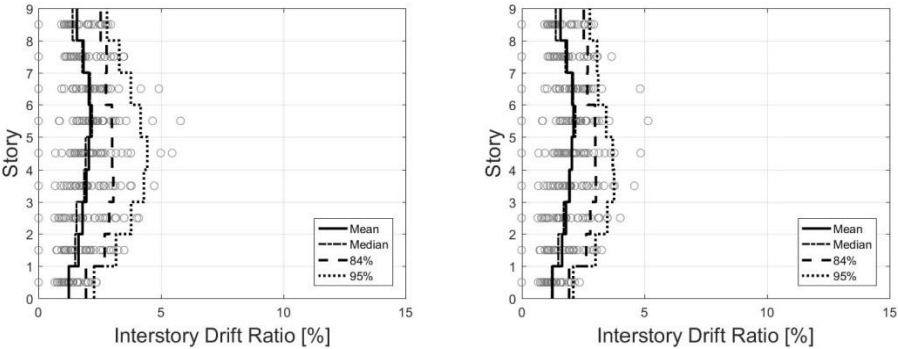


**Figure 4.8: IDR profiles of Models 1 and 3 of 9-Story Building**

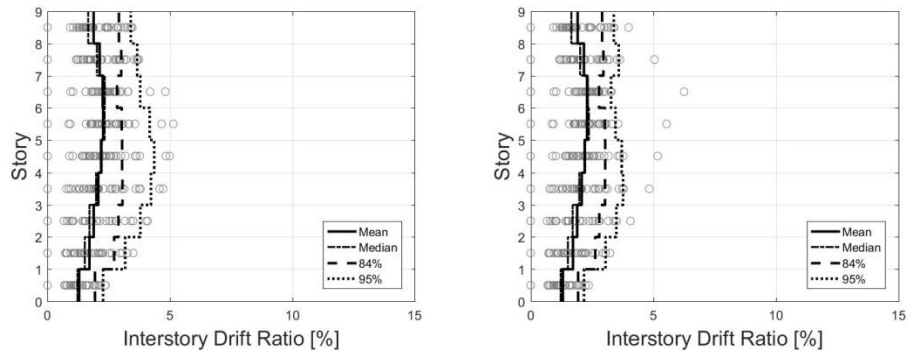


**Figure 4.9: IDR profiles of Models 2 and 4 of 9-Story Building**

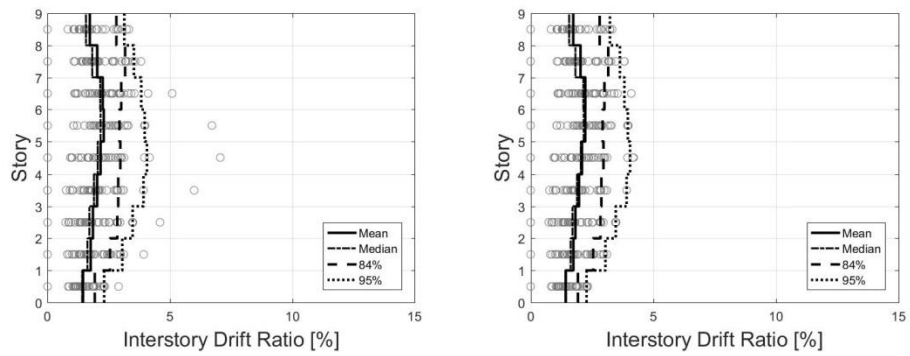


**Figure 4.10: IDR profiles of Models 5 and 7 of 9-Story Building**

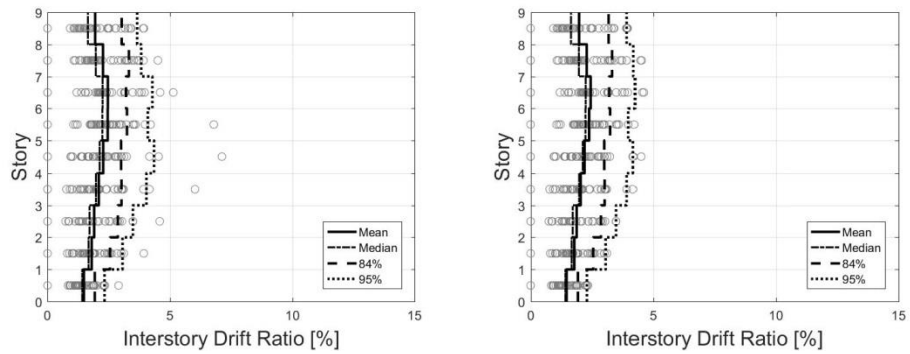


**Figure 4.11: IDR profiles of Models 6 and 8 of 9-Story Building**

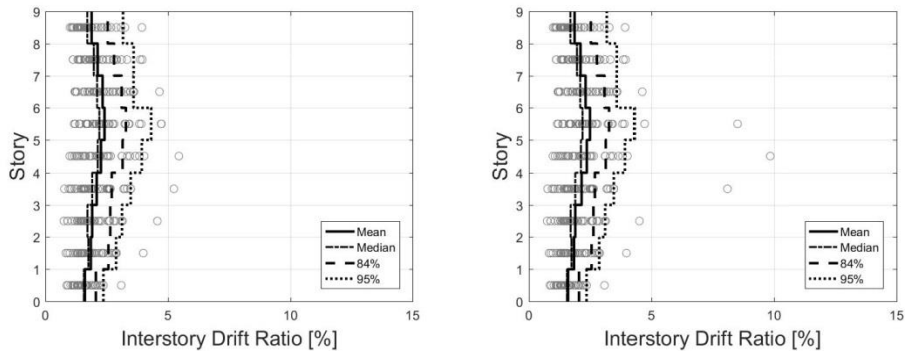


**Figure 4.12: IDR profiles of Models 9 and 11 of 9-Story Building**

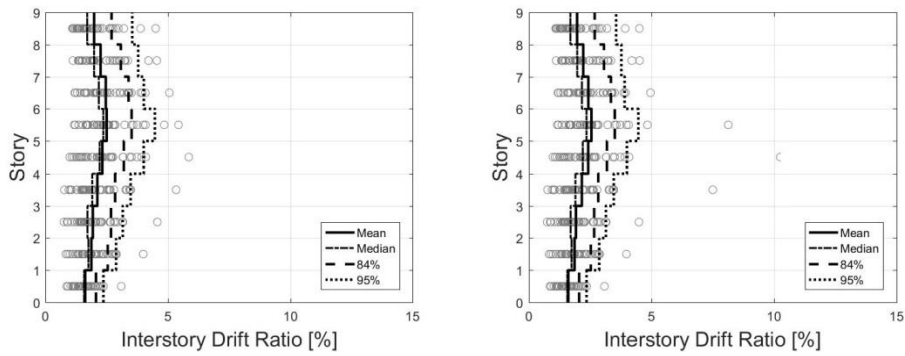


**Figure 4.13: IDR profiles of Models 10 and 12 of 9-Story Building**

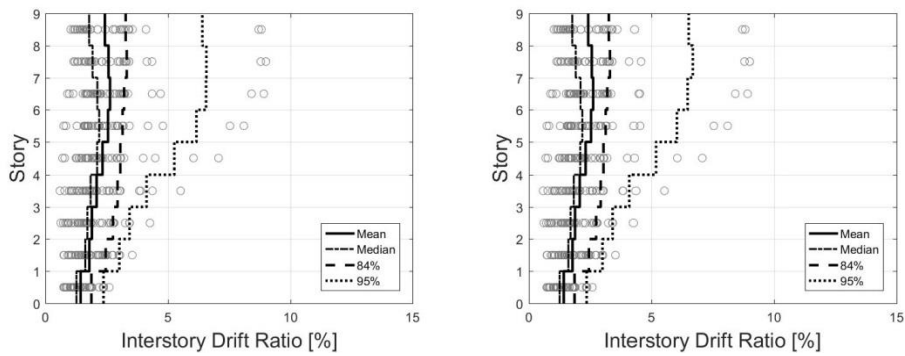


**Figure 4.14: IDR profiles of Models 13 and 15 of 9-Story Building**

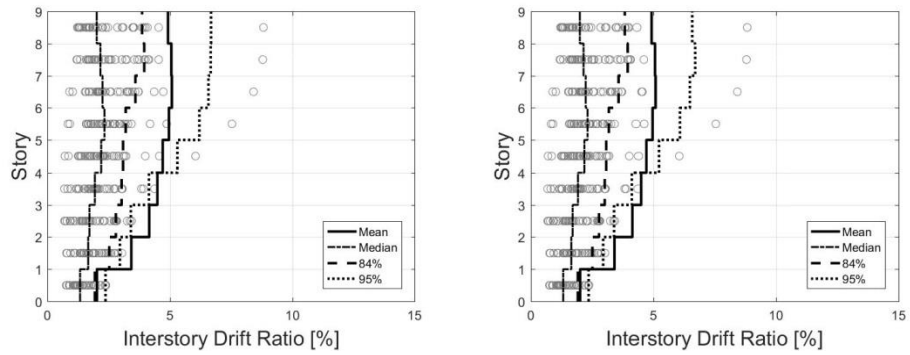


**Figure 4.15: IDR profiles of Models 14 and 16 of 9-Story Building**

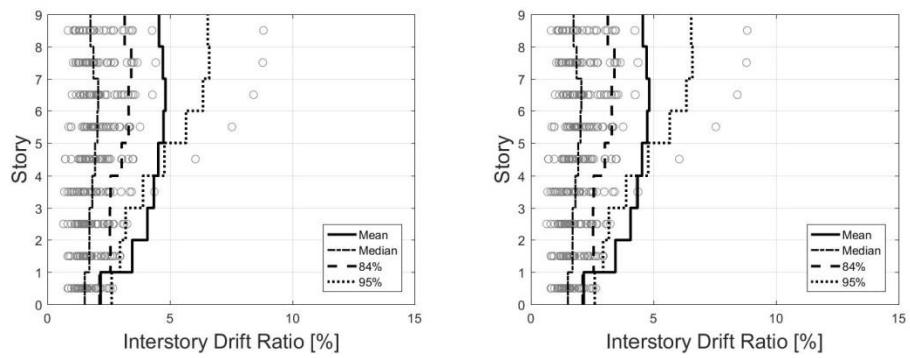


**Figure 4.16: IDR profiles of Models 17 and 19 of 9-Story Building**

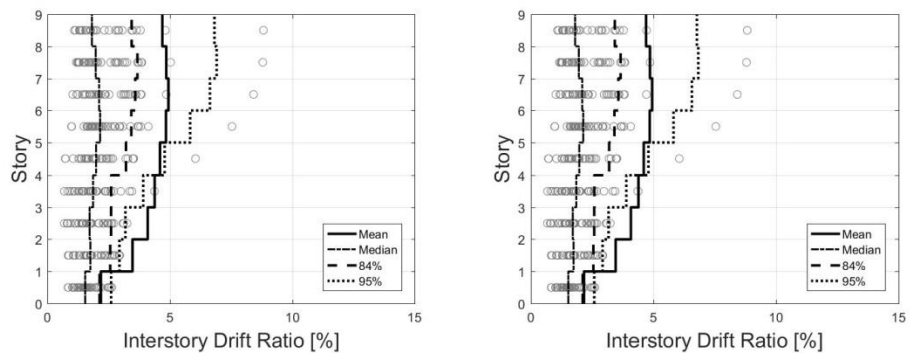


**Figure 4.17: IDR profiles of Models 18 and 20 of 9-Story Building**

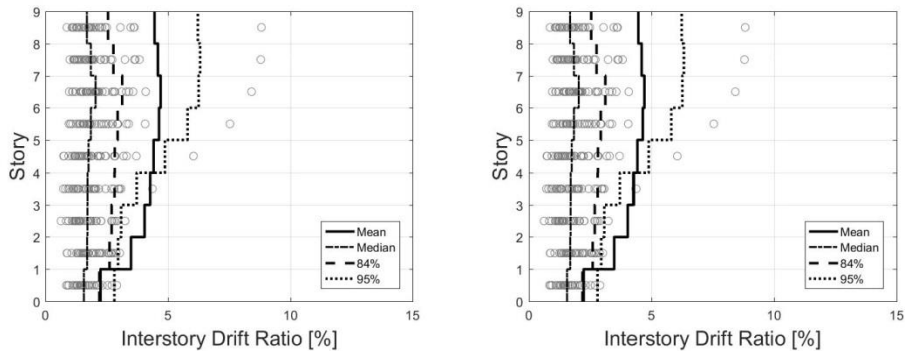


**Figure 4.18: IDR profiles of Models 21 and 23 of 9-Story Building**

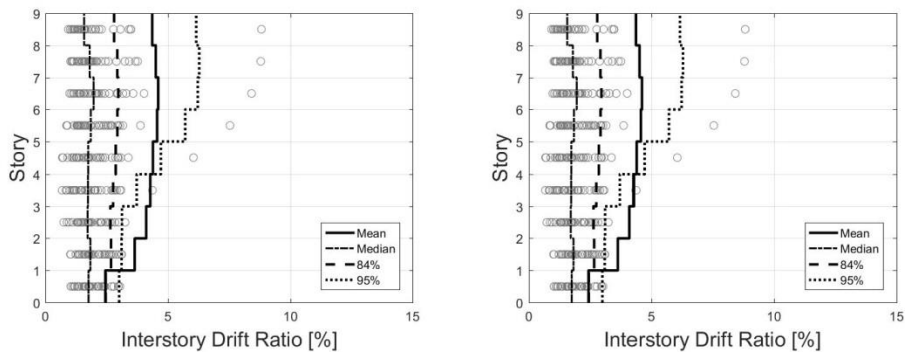


**Figure 4.19: IDR profiles of Models 22 and 24 of 9-Story Building**

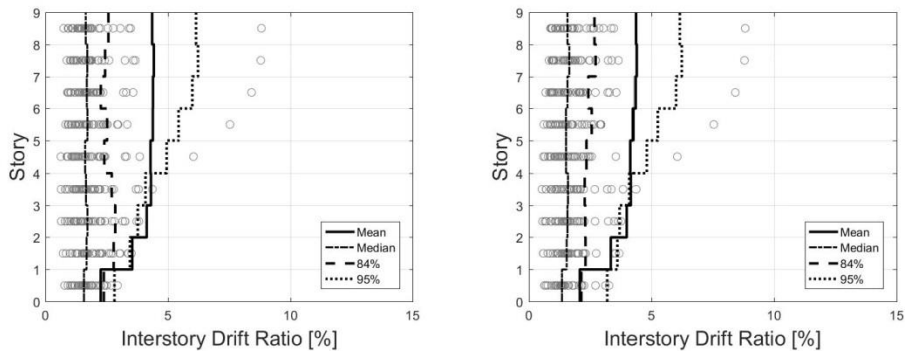


**Figure 4.20: IDR profiles of Models 25 and 26 of 9-Story Building**

Table 4.6 shows the maximum of the median and the 84<sup>th</sup> percentile of the IDR values for 20-story building. All the median values achieve the life safety level of 2.5% and more or less the same level of IDR with the rigid case. However, the 84<sup>th</sup> percentile of IDR values are above the life safety level, but remain below the collapse prevention level of 5%. For the 84<sup>th</sup> percentile IDR values, the models with semi-rigid connections exhibit higher amount of IDR as the moment capacity of the connections even lessens. The presence of severe pinching does not effect the IDR values as compared with the mild pinching cases. For all model cases, the increase due to severe pinching is very small and negligible in most cases. However, pinching had more effect in the 9-story building. Results of the low-rise building from the study by Karakas will be presented next in order to investigate the trends in the nonlinear response as the structure height changes.

**Table 4.6: Maximums of Median and of 84<sup>th</sup> Percentile of IDR Values of the 20-Story Building**

IDR Values of the 20 Story Building				
Model	Median of IDR		84th Percentile	
	$\Delta$ (IDR)	$\Delta_i / \Delta_{rigid}$	$\Delta$ (IDR)	$\Delta_i / \Delta_{rigid}$
1	1.62	0.97	3.22	1.28
2	1.75	1.05	3.31	1.31
3	1.62	0.97	3.50	1.39
4	1.75	1.05	3.50	1.39
5	1.53	0.92	2.96	1.17
6	1.53	0.92	2.96	1.18
7	1.53	0.92	2.96	1.17
8	1.53	0.92	2.96	1.18
9	1.81	1.09	2.65	1.05
10	1.83	1.10	2.65	1.05
11	1.81	1.09	2.65	1.05
12	1.83	1.10	2.65	1.05
13 (Rigid)	1.67	1.00	2.52	1.00

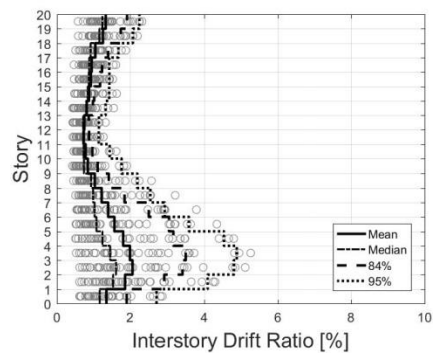
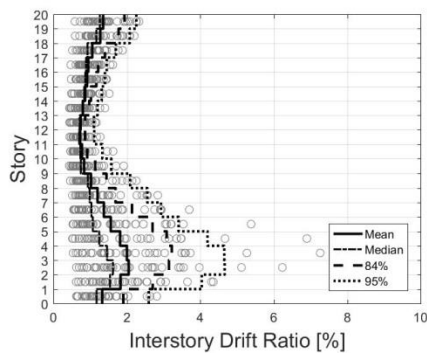


**Figure 4.21: IDR profiles of Models 1 and 3 of 20-Story Building**

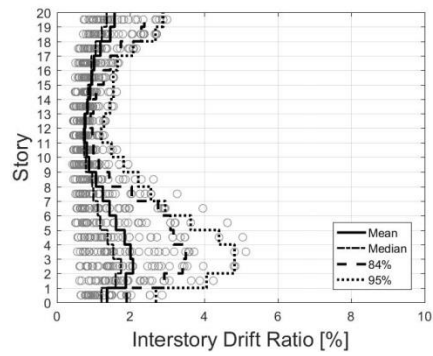
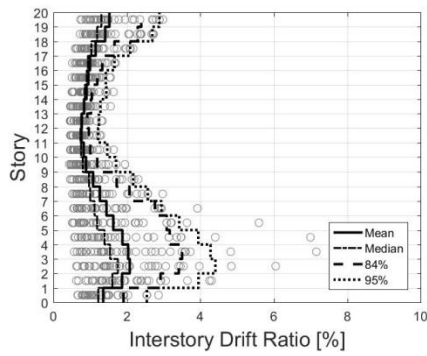


**Figure 4.22: IDR profiles of Models 2 and 4 of 20-Story Building**

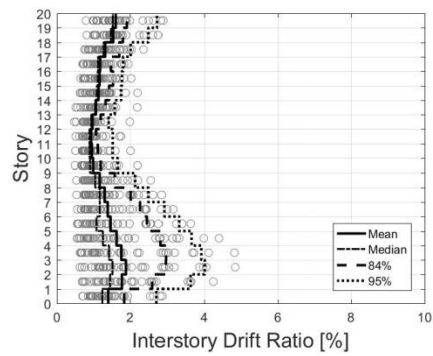
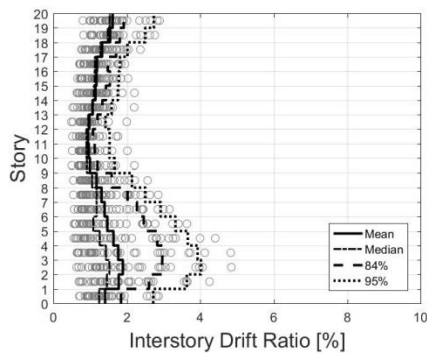


**Figure 4.23: IDR profiles of Models 5 and 7 of 20-Story Building**

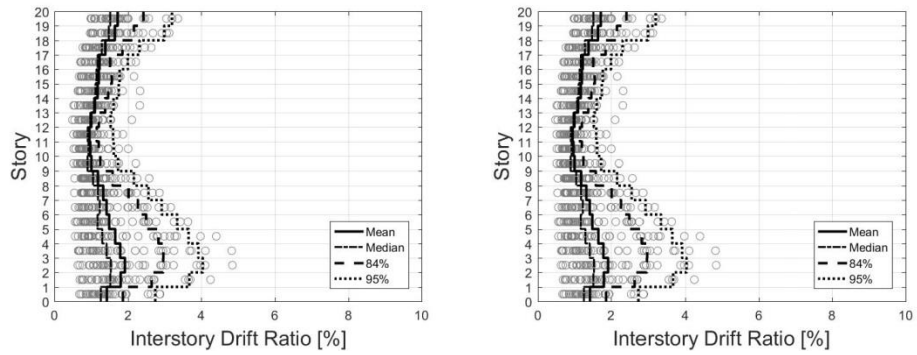


**Figure 4.24: IDR profiles of Models 6 and 8 of 20-Story Building**

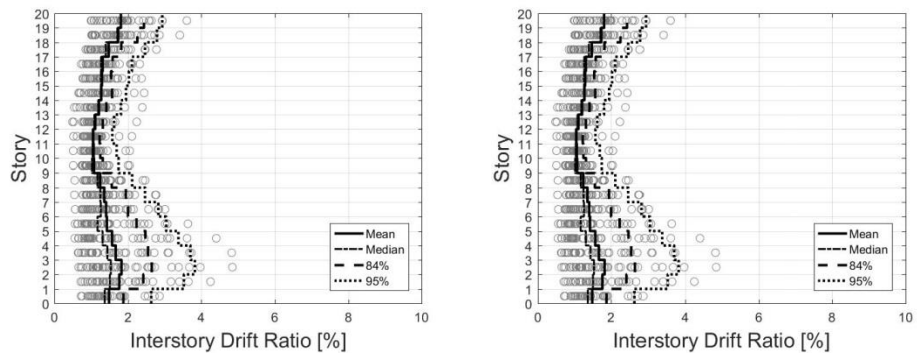


**Figure 4.25: IDR profiles of Models 9 and 11 of 20-Story Building**

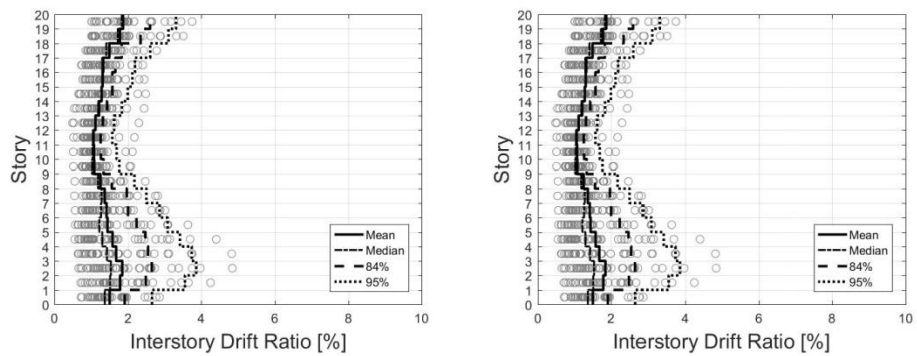


**Figure .26: IDR profiles of Models 10 and 12 of 20-Story Building**

Higher mode effects for 20-story building could also be observed from the IDR profiles shown on above figures.

#### 4.4 Comparison with the Study of Karakas [50]

The maximum of the median and the 84<sup>th</sup> percentile of IDR values of the 3 story building within the study of the Karakas [50] is tabulated below.

All the IDR values of the lower bound design are above the life safety performance level of 2.5%. However, for the upper bound design all the models achieve the level of life safety. Particularly the lower bound design model exhibits larger IDR compared to the rigid case. Furthermore, the change in displacement demands is much more significant for the low-rise building when demands of LB and UB are compared.

**Table 4.7: Maximums of Median of IDR Values of the 3 Story Building by Karakas [50]**

Median of IDR Values of the 3-Story Building						
Lower Bound Design			Upper Bound Design			LB/UB
Models	$\Delta$ (IDR)	$\Delta_i /$ $\Delta_{rigid}$	Models	$\Delta$ (IDR)	$\Delta_i /$ $\Delta_{rigid}$	$\Delta_{LB} /$ $\Delta_{UB}$
1	3.35	1.57	13	2.01	1.15	1.67
2	3.45	1.61	14	2.20	1.25	1.56
3	3.01	1.41	15	2.00	1.14	1.50
4	3.38	1.58	16	2.18	1.24	1.55
5	2.64	1.23	17	1.93	1.10	1.37
6	2.87	1.34	18	1.95	1.11	1.47
7	2.64	1.23	19	1.93	1.10	1.37
8	2.81	1.31	20	1.95	1.11	1.44
9	2.40	1.12	21	1.91	1.09	1.26
10	2.49	1.16	22	1.91	1.09	1.30
11	2.40	1.12	23	1.91	1.09	1.26
12	2.49	1.16	24	1.91	1.09	1.30
25 (Rigid)	2.14	1.00	26 (Rigid)	1.76	1.00	1.22

Table 4.8 shows the 84<sup>th</sup> percentile of IDR values of the 3-story building that has been studied by by Karakas [50]. All the models with the lower bound design exceed the

life safety level of 2.5%, and most of the partial strength cases come very close to the collapse prevention level of 5%, which was not the case for the studied mid-rise and high-rise buildings in this thesis. It is evident that the use of partial strength connections become a more critical issue especially in low-rise steel moment resisting frame buildings and should be approached with more caution. As the structure height increases, the use of partial strength connections as long as connection ductility is ensured, though yields increased displacements, still falls in the safe with regards to the collapse prevention performance level as concluded from the time history analysis. It is worth to recall that in typical steel moment resisting frame design, connections are intended to be protected; however, for the purposes of using connections as an energy dissipation zone, the use of partial strength ductile connections may be possible as a means to dissipate seismic energy for mid-rise to high-rise structures.

**Table 4.8: Maximums of 84<sup>th</sup> percentile of IDR Values of the 3-Story Building by Karakas[50]**

84 <sup>th</sup> Percentile of IDR Values of the 3-Story Building						
Lower Bound Design			Upper Bound Design			LB/UB
Models	$\Delta$ (IDR)	$\Delta_i /$ $\Delta_{rigid}$	Models	$\Delta$ (IDR)	$\Delta_i /$ $\Delta_{rigid}$	$\Delta_{LB} /$ $\Delta_{UB}$
1	4.96	1.30	13	3.90	1.27	1.27
2	5.67	1.48	14	4.11	1.34	1.38
3	4.70	1.23	15	3.60	1.17	1.30
4	4.86	1.27	16	3.96	1.29	1.23
5	4.36	1.14	17	3.84	1.25	1.13
6	4.42	1.16	18	3.87	1.26	1.14
7	4.36	1.14	19	3.84	1.25	1.13
8	4.32	1.13	20	3.87	1.26	1.12
9	4.27	1.12	21	3.64	1.18	1.18
10	4.30	1.12	22	3.73	1.21	1.15
11	4.27	1.12	23	3.64	1.18	1.18
12	4.30	1.12	24	3.73	1.21	1.15
25 (Rigid)	3.83	1.00	26 (Rigid)	3.08	1.00	1.24



## CHAPTER 5

### SUMMARY AND CONCLUSION

This thesis presented the influence of various inherent nonlinear properties that may exist in a connection's behavior on the structural system response of moment resisting frames. In Chapter 1, a brief introduction on the moment resisting frame structural system (SMRF) and beam-column connections was given, and then the literature survey on the partially restrained or also called as semi-rigid connections' response on SMRF was presented. In Chapter 2, description of the analyzed buildings in this thesis, and the structural analysis program and elements and connection models used for the parametric study in this thesis were presented. In Chapter 3, brief discussion on the push-over and the nonlinear time history analysis tools were given and the selected ground motions were presented, and in Chapter 4, the results obtained from parametric study are given. The following are concluded from the parametric study undertaken in this thesis, along with a comparison with the results of low-rise buildings from Karakas [\[50\]](#).

The following conclusions can be stated from the results of the parametric study undertaken in this thesis on the influence of connection nonlinearity to the structural system response of steel moment resisting frame structures.

With regards to nonlinear static (push-over) analysis:

- With respect to the stiffness and strength of a semi-rigid connection, it is observed that strength results in a more pronounced effect on load-versus displacement response of a structure, as observed in push-over curves. When connection stiffness is set to  $15(EI/L)_{\text{beam}}$ , which is 25% lower than the rigid connection idealization threshold of  $20(EI/L)_{\text{beam}}$ , the overall stiffness of the

structure changes roughly in the order of 10-20% for low-rise to high-rise structures. On the other hand, when connection is partial strength and its moment capacity is 30% lower than the beam's plastic capacity, this rendered the overall frame's ultimate capacity drop by a factor of 50% compared with the rigid connection case.

- Along with the geometric effects, overall stability of the structure is highly affected by the presence of strength loss in the moment-rotation response of a connection. For the high rise building, it has been observed that the strength loss could only be tolerated only if the connection's strength is higher than the beam's plastic capacity, however, since the rest of the models fail even before unloading, strength loss at the connection should be approached with great caution as evident from push-over curves.

With regards to the parametric nonlinear time history analysis:

- As a result of increased structural periods, the use of semi-rigid connections allowed for the mid-rise to high-rise structures to attract less seismic forces with respect to the rigid connection case, and therefore, this resulted in an overall smaller increase in the inter-story displacements as the structures' height increases from mid-rise to high-rise; however, for the low-rise structures, this cannot be concluded and inter-story drifts are observed to increase in more pronounced fashion.
- For mid-rise to high-rise structures, the use of semi-rigid connections provided safe performance with regards to life safety prevention limits when the median of the ground motions is considered, which provides the design level response. With regards to an assessment for stronger earthquake response, the performance of these structures all passed life safety but stayed well below collapse prevention limits for all semi-rigid connection cases. Therefore, as long as connection ductility is ensured, presence of semi-rigid connection response still maintains the structural system response of especially high-rise structures within performance limits.

- For the low-rise structures, semi-rigid connection response caused more pronounced inter-story displacement demands, where the life safety limits are mostly overpassed for most connection response cases. With regards to the collapse prevention limit, the nonlinear response characteristic of the connections become a more critical issue in maintaining structural system response within safety limits for the low-rise buildings.
- The level of pinching is observed to cause an overall increase on structural displacements that may be especially critical for the low-rise buildings to go over performance safety limits more easily. However, for mid-rise to high-rise buildings, pinching alone is not observed to be a major parameter that provides a safety judgement on performance limits.
- Use of partial strength connections caused more significant increase in the inter-story displacements of the low-rise buildings than the mid-rise to high-rise buildings. It is therefore concluded that the use of partial strength connections that satisfy ductility requirements does not alter the performance limit criteria, and can be especially chosen as a means to dissipate and localize seismic energy dissipation at connection zone for mid-rise to high-rise structures.



## REFERENCES

- [1] A. Elnashai, V. Papanikolaou, and D. Lee. Zeus-NL A system for inelastic analysis: User Manual. 2008.
- [2] A. Gupta and H. Krawinkler. Seismic demands for the performance evaluation of steel moment resisting frame structures. Technical report, The John A. Blume Earthquake Engineering Center, Department of Civil and Environmental Engineering, Stanford University. Report No. 132, 1999.
- [3] A. Pirmoz and M. M. Liu. Direct displacement-based seismic design of semi-rigid steel frames. *Journal of Constructional Steel Research*, 128:201- 209, 2017.
- [4] A. S. Elnashai and A. Y. Elghazouli. Seismic behavior of semi-rigid steel frames. *Journal of Constructional Steel Research*, 29(1-3):149-174, 1994.
- [5] A. Saritas, A. Koseoglu; "Distributed Inelasticity Planar Frame Element with Localized Semi-Rigid Connections for Nonlinear Analysis of Steel Structures", *International Journal of Mechanical Sciences* Vol. 96-97, pp.216-231, 2015.
- [6] Abolmaali A. Nonlinear dynamic finite element analysis of steel frames with semi-rigid joints. Norman, OK, USA: University of Oklahoma; 1999.
- [7] Akshay G., Helmut K. "Seismic Demands for Performance Evaluation of Steel Moment Resisting Frame Structures" The John A. Blume Earthquake Engineering Center, Department of Civil and Environmental Engineering Stanford University, Report No.132 (June, 1999).

- [8] American Institute of Steel Construction, Inc. AISC 341-10. Seismic Provisions for Structural Steel Buildings, 2010.
- [9] American Institute of Steel Construction, Inc. AISC 360-10. Specification for Structural Steel Buildings, 2010.
- [10] Ansys Inc. ANSYS Fluent UDF Manual. Knowledge Creation Diffusion Utilization, 15317(November):724-746, 2013.
- [11] B. F. Maison and K. Kasai. SAC/BD-99/16. Seismic Performance of 3 and 9 Story Partially Restrained Moment Frame Buildings. Technical report, SAC Joint Venture, 2000.
- [12] Balendra T., Huang X. “Overstrength and Ductility Factors for Steel Frames Designed According to BS 5950” Journal of Structural Engineering 2003.129:1019-1035.
- [13] Chen W F, Yamaguchi E. Spotlight on steel moment frames. Civil Engineering, ASCE, 1996, 44–46.
- [14] D. A. Foutch. FEMA 355F. State of the Art Report on Performance Prediction and Evaluation of Steel Moment-Frame Buildings. Technical report, Federal Emergency Management Agency (FEMA), 2000.
- [15] Driscoll G.C. “Elastic-plastic Analysis of Top-and Seat-Angle Connections” Journal of Constructional Steel Research 8,119-136 (1987).
- [16] E. Lui and W. Chen. Steel frame analysis with flexible joints. Journal of Constructional Steel Research, 8:161-202, 1987.
- [17] E. M. Lui and W. F. Chen. Analysis and behavior of flexibly-jointed frames. Engineering Structures, 8(2):107-118, 1986.

- [18] Eurocode 3: Design of steel structures - Part 1-8: Design of joints (2005).
- [19] F. A. Charney, H. Iyer, and P. W. Spears. Computation of major axis shear deformations in wide flange steel girders and columns. *Journal of Constructional Steel Research*, 61(11):1525 \_ 1558, 2005.
- [20] FEMA 356. *Prestandard and Commentary for the Seismic Rehabilitation of Buildings*. Technical report, American Society of Civil Engineers, Washington, DC, 2000.
- [21] Frye M.J. and Morris G.A. "Analysis of Flexibly Connected Steel Frames" *Can. Journal of Civil Engineers* Vol2, 280-291 (1975).
- [22] H. Krawinkler and G.D.P.K. Seneviratna. Pros and Cons of Push-over Analysis of Seismic Performance Evaluation. *Engineering Structures*, 20(4), 452-464, 1998.
- [23] H.F. Ozel, A. Saritas, T. Tasbahji; "Consistent matrices for steel framed structures with semi-rigid connections accounting for shear deformation and rotary inertia effects", *Engineering Structures*, Vol. 137, pp. 194-203, 2017.
- [24] Izzuddin and Elnashai. ADAPTIC-A Program for Adaptive Large Displacement Elastoplastic Dynamic Analysis of Steel, Concrete and Composite Frames. Report No. ESEE, 7:89, 1989.
- [25] K. Lee and D. A. Foutch. SAC/BD-00/25. *Performance Prediction and Evaluation of Steel Special Moment Frames for Seismic Loads*. Technical report, SAC Joint Venture, 2000.
- [26] Kishi, N., Chen W.F., Goto Y. and Matsuoka K.G. "Applicability of Three-Parameter Power Model to Structural Analysis of Flexibly Jointed Frames"

- Proceedings of Mechanics Computing in 1990's and beyond, H.Adeli and R.L.Sierakowski eds.,Columbus, Ohio U.S.A, May20-22,233-237 (1991).
- [27] Krishnamurthy N., Huang H.T., Jefferey P.K. and Avery L.K. "Analytical M- $\theta$  Curves for End-plate Connections", ASCE,105 (ST1),133-145 (1979) .
- [28] Kukreti A.R., Murray T.M. and Abolmali A. "End-plate Connection Moment-Rotation Relationship" Journal of Constructional Steel Research 8,137-157 (1987).
- [29] Kurt H. Gerstle "Effect of Connections on Frames" J. Construct. Steel Research 10 (1988) 241-267.
- [30] Maison B.F., Kasai K., Mayangarum A. "Effects of Partially Restrained Connection Stiffness and Strength on Frame Seismic Performance" SAC Steel Project-Report No.SAC/BD-99/17-(June, 2000).
- [31] Mwafy, A.M., Elnashai, A.S. "Static push-over versus dynamic collapse analysis of RC buildings", (2001) Engineering Structures, 23 (5), pp. 407-424.
- [32] N. D. Aksoylar, A. S. Elnashai, and H. Mahmoud. The design and seismic performance of low-rise long-span frames with semi-rigid connections. Journal of Constructional Steel Research, 67(1):114-126, 2011.
- [33] Nogueiro P, da Silva LS, Bento R, Simoes R. Numerical implementation and calibration of a hysteretic model with pinching for the cyclic response of steel joints. Adv Steel Constr 2007;3(1):459-84.
- [34] P. Somerville, N. Smith, S. Punyamurthula, and J. Sun. SAC/BD-97/04. Development of ground motion time histories for phase 2 of the FEMA/SAC steel project. Technical report, Report No. SAC/BD-97/04, 1997.

- [35] Patel K.V. and Chen W.F. "Nonlinear Analysis of Steel Moment Connections" ASCE 110(ST8), 1861-1874 (1984).
- [36] R. Allahabadi and G. H. Powell. DRAIN-2DX user guide. University of California, Earthquake Engineering Research Center, 1988.
- [37] R. Bjorhovde, A. Colson, and J. Brozzetti. Classification System for Beam-to-Column Connections. Journal of Structural Engineering (United States), 116(11):3059-3076, 1990.
- [38] Ramberg W, Osgood WR. Description of stress-strain curves by three parameters. Washington DC: National Advisory Committee for Aeronautics; 1943.
- [39] Recommended seismic design criteria for new steel moment-frame buildings, FEMA 350, 2000.
- [40] Richard R.M., Gillet P.E.,Kriegh J.D.,and Lewis B.A. "The Analysis and Design of Single Plate Framing Connections" AISC Engrg.J.2nd Quarter,38-52.
- [41] Richard RM, Abbott BJ. Versatile elasto-plastic stress-strain formula. J Eng Mech Div ASCE 1975;101(EM4):511-5.
- [42] S. Mazzoni, F. McKenna, M. H. Scott, G. L. Fenves, et al. OpenSees Command Language Manual. Pacific Earthquake Engineering Research (PEER) Center, 2006.
- [43] Saritas, A., Soydas, O., Variational Base and Solution Strategies for Nonlinear Force-Based Beam Finite Elements", International Journal of Non-Linear Mechanics, Vol. 47, no. 3, pp. 54-64, 2012.

- [44] Sekulovic M, Salatic R. Nonlinear analysis of frames with flexible connections. *Comput Struct* 2001;79(11):1097–107.
- [45] Shohara, R., Sawamoto, Y., Imai, K., Nakazawa, H., Narihara, H., & Fukumoto, T. Strength and ductility of non-embedded steel reinforced concrete column base, *Journal of Advanced Concrete Technology*, Volume 5, Issue 2, June 2007, Pages 223-234.
- [46] Valipour HR, Bradford M. An efficient compound-element for potential progressive collapse analysis of steel frames with semi-rigid connections. *Finite Elem Anal Des* 2012:35–4860 2012:35–48.
- [47] Vamvatsikos, D., and Cornell, C. A.(2002). “Incremental dynamic analysis.” *Earthquake Eng. Struct. Dyn.*, 31(3), 491–514.
- [48] W.-F. Chen, N. Kishi, and M. Komuro. *Semi-Rigid Connections Handbook*. J. Ross Publishing civil & environmental engineering series. Ft. Lauderdale, FL : J. Ross Pub., c2011., 2011.
- [49] W.-F. Chen. *Practical Analysis for Semi-Rigid Frame Design*. Singapore River Edge, NJ : World Scientific, c2000., 2000.
- [50] Z. Karakaş. " Influence of the nonlinear behavior of semi-rigid connections on the analysis of low-rise steel framed structures" Master's thesis, Middle East Technical University, Ankara, Turkey, January 2017.